MOLECULAR AND CELLULAR BIOLOGY, Nov. 1996, p. 6603–6616 Vol. 16, No. 11
0270-7306/96/$04.00+0

Identification of a Regulatory Subcomplex in the Guanine Nucleotide Exchange Factor eIF2B That Mediates Inhibition by Phosphorylated eIF2

WEIMIN YANG AND ALAN G. HINNEBUSCH*

Laboratory of Eukaryotic Gene Regulation, National Institute of Child Health and Human Development, Bethesda, Maryland 20892-2785

Received 17 June 1996/Returned for modification 30 July 1996/Accepted 20 August 1996

Eukaryotic translation initiation factor 2B (eIF2B) is a five-subunit complex that catalyzes guanine nucleotide exchange on eIF2. Phosphorylation of the α subunit of eIF2 [creating eIF2(αP]) converts eIF2 · GDP from a substrate to an inhibitor of eIF2B. We showed previously that the inhibitory effect of eIF2(αP) can be decreased by deletion of the eIF2B α subunit (encoded by *GCN3*) and by point mutations in the β and δ subunits of eIF2B (encoded by *GCD7* and *GCD2*, respectively). These findings, plus sequence similarities among GCD2, GCD7, and GCN3, led us to propose that these proteins comprise a regulatory domain that interacts with eIF2(αP) and mediates the inhibition of eIF2B activity. Supporting this hypothesis, we report here that overexpression of GCD2, GCD7, and GCN3 specifically reduced the inhibitory effect of eIF2(αP) on translation initiation in vivo. The excess GCD2, GCD7, and GCN3 were coimmunoprecipitated from cell extracts, providing physical evidence that these three proteins can form a stable subcomplex. Formation of this subcomplex did not compensate for a loss of eIF2B function by mutation and in fact lowered eIF2B activity in strains lacking eIF2(αP). These findings indicate that the trimeric subcomplex does not possess guanine nucleotide exchange activity; we propose, instead, that it interacts with eIF2(αP) and prevents the latter from inhibiting native eIF2B. Overexpressing only GCD2 and GCD7 also reduced eIF2(αP) toxicity, presumably by titrating GCN3 from eIF2B and producing the four-subunit form of eIF2B that is less sensitive to eIF2(αP). This interpretation is supported by the fact that overexpressing GCD2 and GCD7 did not reduce eIF2(αP) toxicity in a strain lacking *GCN3*; however, it did suppress the impairment of eIF2B caused by the *gcn3^c-R104K* mutation. An N-terminally truncated GCD2 protein interacted with other eIF2B subunits only when GCD7 and GCN3 were overexpressed, in accordance with the idea that the portion of GCD2 homologous to GCD7 and GCN3 is sufficient for complex formation by these three proteins. Together, our results provide strong evidence that GCN3, GCD7, and the C-terminal half of GCD2 comprise the regulatory domain in eIF2B.

One of the best-characterized mechanisms for regulating the rate of protein synthesis in eukaryotic cells involves phosphorylation of translation initiation factor 2 (eIF2) and down-regulation of eIF2B, the guanine nucleotide exchange factor for eIF2. eIF2 plays a central role in translation initiation, forming a ternary complex with GTP and charged initiator $tRNA^{Met}$ that delivers the Met-$tRNA_i^{Met}$ to 40S ribosomes. Following recognition of the AUG codon by $tRNA_i^{Met}$, the GTP in the ternary complex is hydrolyzed and eIF2 is released in a binary complex with GDP. To re-form the ternary complex and participate in subsequent rounds of initiation, eIF2 must be recycled from the GDP-bound form to the GTP-bound form, and this guanine nucleotide exchange reaction is catalyzed by eIF2B. Phosphorylation of the α subunit of eIF2 on serine 51 [creating eIF2(αP)] inhibits nucleotide exchange by eIF2B; in addition, eIF2(αP) interferes with the recycling of nonphosphorylated eIF2 by eIF2B. According to one proposed mechanism, dissociation of the eIF2B · eIF2(αP) · GDP complex is extremely slow, and thus eIF2B is bound irreversibly by phosphorylated eIF2. Because eIF2 is present in considerable excess of eIF2B, this mechanism can explain how phosphorylation of a small proportion of eIF2 is sufficient to sequester all of the eIF2B in inactive complexes (25). Alternatively, it has been suggested that eIF2(αP) has a much greater association rate with eIF2B than does nonphosphorylated eIF2, allowing eIF2(αP) to interfere with the recycling of nonphosphorylated eIF2 as a competitive inhibitor without forming a long-lived eIF2B · eIF2(αP) · GDP complex (30). This latter hypothesis is more consistent with the in vivo effects of overproducing eIF2 in yeast cells, in which case it was found that the ratio of phosphorylated to nonphosphorylated eIF2 was more important than the absolute amount of eIF2(αP) in determining the extent of eIF2B inhibition (11). Little is known at the molecular level about how phosphorylation of eIF2 affects its affinity for eIF2B or how eIF2(αP) interferes with nucleotide exchange by eIF2B.

Three protein kinases, HRI, PKR, and GCN2, that specifically phosphorylate Ser-51 under different stress conditions have been identified (19). HRI and PKR (also known as DAI and p68 kinase) phosphorylate eIF2 in mammalian cells to an extent that shuts off total protein synthesis by complete inhibition of eIF2 recycling by eIF2B. In *Saccharomyces cerevisiae*, GCN2 phosphorylates eIF2 in response to starvation for amino acids or purines by an amount that does not inhibit total protein synthesis but does lead to a specific increase in translation of *GCN4* mRNA. *GCN4* encodes a transcriptional activator of genes encoding amino acid biosynthetic enzymes. Translation of *GCN4* mRNA is inversely coupled to the concentration of eIF2 · GTP · Met-$tRNA_i^{Met}$ ternary complexes by the presence of four small open reading frames (uORFs) in

* Corresponding author. Mailing address: Laboratory of Eukaryotic Gene Regulation, National Institute of Child Health and Human Development, Bldg. 6B, Room 3B-309, 6 Center Dr., Bethesda, MD 20892-2785. Phone: (301) 496-4480. Fax: (301) 496-0243. Electronic mail address: ahinnebusch@NIH.GOV.

the *GCN4* mRNA leader. Translation of these uORFs prevents ribosomes from reaching the *GCN4* start codon in nonstarved cells. Phosphorylation of eIF2 under starvation conditions reduces the abundance of ternary complexes, enabling ribosomes to bypass the uORFs and initiate translation at *GCN4* instead (21). Mutationally activated forms of GCN2 that generate much higher amounts of eIF2(αP) than are seen in starved wild-type yeast cells have been isolated. In these *GCN2^c* mutants (10, 28) or in yeast cells expressing human PKR (5, 9), general translation and cellular growth are also greatly inhibited.

All five subunits of eIF2B, encoded by *GCD6* (ε), *GCD2* (δ), *GCD1* (γ), *GCD7* (β), and *GCN3* (α), were first identified genetically by mutations that impair *GCN4* translational control. The four *GCD* genes encoding eIF2B subunits are essential, and nonlethal mutations in each that result in derepressed levels of *GCN4* translation (Gcd$^-$ phenotype) and reduced cellular growth on nutrient-rich medium have been obtained. These *gcd* mutations presumably lead to decreased concentrations of the ternary complex independently of eIF2 phosphorylation by impairing the catalytic activity of eIF2B. In contrast, the *GCN3*-encoded subunit of eIF2B is dispensable, and its inactivation in otherwise wild-type strains impairs only the ability to stimulate *GCN4* translation under starvation conditions. This is the same (Gcn$^-$) phenotype observed upon inactivation of the protein kinase GCN2 or the replacement of Ser-51 in eIF2α with nonphosphorylatable alanine. On the basis of this finding, it was proposed that GCN3 is a regulatory subunit of eIF2B required to mediate the inhibitory effect of eIF2(αP) on eIF2B function (21). In accord with these interpretations of mutant phenotypes, it was shown recently that the effects of eIF2 phosphorylation on *GCN4*-specific and general translation initiation are reversed by overproducing all five subunits of eIF2B or, even more effectively, by overexpressing a four-subunit complex containing the essential proteins GCD6, GCD2, GCD1, and GCD7 but lacking GCN3 (11). These results confirmed that eIF2B function is impaired in yeast cells when eIF2 is phosphorylated on Ser-51 and lent further support to the idea that GCN3 makes eIF2B more sensitive to the inhibition by eIF2(αP).

In addition to GCN3, the *GCD7*- and *GCD2*-encoded subunits of eIF2B have important roles in the regulation of eIF2B by eIF2(αP). GCD7 and GCN3 are similar in sequence over nearly their entire lengths, and the C-terminal half of GCD2 is similar in sequence to both GCD7 and GCN3 (3, 26). These sequence similarities raise the possibility that GCD7 and GCD2 act in concert with GCN3 to mediate the inhibition of eIF2B by eIF2(αP). This idea was supported by the isolation of point mutations in *GCD7* and *GCD2* that reverse the toxicity of eIF2 phosphorylation on cell growth. These mutations appear to have no effect on eIF2B catalytic activity but decrease its ability to be inhibited by eIF2(αP) (35). More recently, saturation mutagenesis of *GCD2*, *GCD7*, and *GCN3* has shown that the critical regulatory sites in GCD2 are located in the C-terminal half of the protein, which is related in sequence to GCD7 and GCN3. Moreover, some of the regulatory mutations map to similar, or even identical, positions in all three proteins, particularly in the extreme C-terminal segments where the sequence identity is greatest. These results strongly suggest that structurally similar segments in GCD2, GCD7, and GCN3 are involved in their regulatory functions, implying that these functions are closely related. We suggested that regulatory segments in each protein are involved in making subunit-specific contacts with eIF2α in the vicinity of the phosphorylation site and that contacts made by each protein are required to mediate the inhibitory effects of eIF2(αP) on eIF2B catalytic activity (27).

By analogy with other multisubunit-regulated enzymes that contain regulatory and catalytic subunits, e.g., cyclic AMP-dependent protein kinase (34), we reasoned that the GCD2, GCD7, and GCN3 subunits might physically interact with one another in eIF2B and comprise a regulatory domain that directly interacts with the phosphorylated α subunit of eIF2. If this were true, it might be possible to prevent eIF2(αP) from inhibiting eIF2B by individually overproducing GCD2, GCD7, or GCN3. Alternatively, if GCD2, GCD7, and GCN3 comprise a surface that contacts eIF2α at several points, it might be necessary to overproduce two of the three or all three proteins simultaneously to neutralize the inhibitory effects of eIF2(αP) on translation initiation. If GCD1 and GCD6 comprised the catalytic core of eIF2B, then overexpression of only these subunits might produce a functional eIF2B complex that is insensitive to inhibition by eIF2(αP). In this study, we tested these predictions by overexpressing numerous combinations of eIF2B subunits and examining each for the ability to suppress the growth-inhibitory effects of eIF2 phosphorylation catalyzed by a GCN2^c kinase. We found that overexpressing GCD2, GCD7, and GCN3 in yeast cells led to formation of a stable subcomplex containing these three proteins that substantially reduced the growth-inhibitory effects of eIF2(αP). We present evidence that the overexpressed GCD2-GCD7-GCN3 trimeric subcomplex did not increase the level of functional eIF2B in the absence of the inhibitor eIF2(αP), nor did it reduce the level of eIF2 phosphorylation in the cell. Together, these results strongly suggest that the trimeric subcomplex can sequester eIF2(αP) and prevent it from inhibiting native eIF2B. We also present genetic and biochemical evidence that the C-terminal portion of GCD2, which is similar in sequence to GCD7 and GCN3, is sufficient for interaction with GCD7 and GCN3. These findings support the idea that GCN3, GCD7, and the C-terminal half of GCD2 comprise a regulatory subdomain in eIF2B that interacts with eIF2 and mediates the inhibitory effects of eIF2(αP) on eIF2B catalytic activity.

MATERIALS AND METHODS

Yeast strains and genetic methods. Standard methods were used for transformation (22) and genetic manipulation (32) of yeast strains. Methods used for testing sensitivity to the amino acid analogs 3-aminotriazole (3-AT) and 5-fluoro-DL-tryptophan (5-FT) have been described previously (18). The yeast strains used in this work were H1402 (*MAT*α *leu2-3 leu2-112 ura3-52 ino1*) (14), H1608 (*MAT*α *leu2-3 leu2-112 ura3-52 ino1 GCN2^c-M719V-E1537G HIS4-lacZ*) (28), H1489 (*MAT*α *leu2-3 leu2-112 ura3-52 gcn3^c-R104K*) (14), H1728 (*MAT*α *leu2-3 leu2-112 ura3-52 gcd6-1*) (3), BJ1995 (*MAT*α *leu2 ura3-52 trp1 gal2 pep4-3 prb1-1122*) (23), GP3040 (*MAT***a** *leu2-3 leu2-112 ura3-52 trp1-Δ63 gcd2Δ::hisG* bearing plasmid pCP62 containing *URA3* and *GCD2*) (27), and GP3153 (*MAT***a** *leu2-3 leu2-112 ura3-52 trp1-Δ63 gcn3Δ::LEU2*) (27). Strain H2526 (*MAT*α *leu2-3 leu2-112 ura3-52 ino1 HIS4-lacZ gcn2Δ*) was constructed by a two-step gene disruption of *GCN2* in strain H1402 as follows. Plasmid p1144, an integrating *URA3* plasmid containing a *gcn2Δ* allele (10), was digested with *Bst*EII and used to transform H1402 to Ura$^+$. The transformants were grown on 5-fluoroorotic acid plates (29), and strain H2526 was isolated as a Ura$^-$ derivative showing a 3-AT-sensitive phenotype. Strains H1402, H1608, H1489, and H2526 are isogenic.

The various plasmid-borne *HA-GCD2* alleles shown in Fig. 8A were tested for complementation of the lethal phenotype of a chromosomal deletion of *GCD2* by introducing them into strain GP3040, containing chromosomal *gcd2Δ* and *GCD2* on a *URA3*-containing plasmid, and culturing the resulting transformants on 5-fluoroorotic acid plates. Only the transformants containing hemagglutinin gene (*HA*)-tagged *GCD2*(*Δ4-26*) or a plasmid bearing untagged *GCD2* were able to grow on 5-fluoroorotic acid medium, indicating that the episomal wild-type *GCD2* was essential for growth in the strains containing truncations in *GCD2* to residue 189, 288, or 403.

Plasmids. pRS425 and pRS426 are 2μm plasmids described previously (6) and pJB115 (3). Plasmid p1873 is a derivative of pRS425 containing *GCD1* and *GCD6*, p1871 is a derivative of pRS426 that contains *GCD2*, *GCD7*, and *GCN3*, and p1872 contains only *GCD2* and *GCD7*. All three plasmids were described previously (11). Plasmid p1421 (9) encoding human PKR-K296R mutant kinase

was described previously. Plasmid p1545, encoding wild-type PKR, was constructed by inserting the *Apa*I-*Pst*I fragment containing PKR isolated from p1420 (9) between the *Apa*I and *Pst*I sites of pRS425 (28a). Plasmid p2298 was constructed by ligating the 2.1-kb *Eag*I-*Eco*RI *GCD7* fragment (11) with the 4.0-kb *Eco*RI-*Bam*HI *GCN3* fragment from Ep69 (14) and *Eag*I-*Bam*HI-digested pRS426. p2299 was constructed by removing *GCD7* from p1871 by digesting with *Spe*I and then religating the 1.9-kb *GCN3* fragment with the 8.0-kb fragment containing *GCD2* and the pRS426 vector DNA. p2297 was made by religating *Not*I-cleaved p1871 to remove *GCD7* and *GCN3*. p2304 was created by digesting p1871 with *Nhe*I and *Xho*I to remove *GCD2* and *GCD7*, end filling the fragment with Klenow polymerase, and religating. p2305 was created by digesting p2298 with *Eco*RI to remove *GCN3* and leave only *GCD7*. p1874, was constructed by subcloning the 2.6-kb *Eag*I-*Cla*I *GCD2* fragment into pRS425.

Plasmids p1875, p1876, p1877, and p1878 were derived from p1874 by progressive truncation of the *GCD2* coding sequences from the N terminus, beginning with the fourth codon, and fusion of the hemagglutinin (HA) epitope tag (13) at the deletion junction. Construction of these plasmids involved the following four steps: (i) isolation of a 126-bp *Bgl*II-*Pst*I fragment containing 61 bp of the 5′ untranslated leader of *GCD2* mRNA, the first three codons (Met-Ser-Gly) of *GCD2*, and the coding sequences for the HA epitope (Tyr-Pro-Tyr-Asp-Val-Pro-Asp-Tyr-Ala) (this fragment was prepared by PCR amplification of the 5′ region of *GCD2* by using the top-strand primer D2 [5′GATAATCAGC GTAAGTGCAT A*AGATC*3′ {italics indicate a portion of the *Bgl*II site}] and the bottom-strand primer D2HA [5′GTCCCGGAT C*CTGCAG*CGT AATCTG GAAC ATCGTATGGG TA**GCCGCTCA T**AGCAATTTG ATTATCGACG C3′ {boldface and underlining indicate the sequences encoding the first three amino acids of GCD2 and the HA epitope, respectively}]); the PCR-amplified fragment was digested with *Bgl*II and *Pst*I); (ii) isolation of 9.0- and 9.5-kb fragments produced by digesting p1874 completely with *Bgl*II and partially with *Pst*I; (iii) ligating the 126-bp PCR-amplified DNA with the 9.0- and 9.5-kb DNA fragments described in step ii to create p1875 and p1876, respectively; and (iv) confirming the sequence of the 126-bp PCR-amplified fragments in p1875 and p1876 by the dideoxyribonucleotide chain termination method (31). p1877 was derived from p1875 by digestion with *Pst*I and *Bam*HI, end filling with Klenow fragment in the presence of dGTP, dATP, and dTTP (dCTP was omitted to produce an in-frame fusion at the deletion junction in the *GCD2* coding sequence), and religation. p1878 was constructed by digesting p1875 with *Nde*I and *Pst*I, end filling with Klenow fragment in the absence of deoxyribonucleotide triphosphates (in order to construct an in-frame fusion at the deletion junction in *GCD2*), and religation. p2234, which encodes residues 1 to 323 of *Escherichia coli* TrpE fused to residues 136 to 288 of GCD2, was produced by *Bam*HI and *Cla*I digestion of p748 (26), end filling with Klenow fragment in the presence of all four deoxyribonucleotide triphosphates, and religation. p1999 was constructed by inserting the 4.0-kb *Eco*RI-*Bam*HI *GCN3* DNA fragment (14) into pRS425. Plasmid p2339 was made by subcloning the 8.0-kb *Sal*I-*Xba*I fragment containing the *GCN2^c-516* allele from p1056 (28) onto the low-copy-number *TRP1* plasmid pRS314 (33).

Immunoblot analysis of strains overexpressing subunits of eIF2B. Transformants of strain H1402 containing the appropriate plasmids were grown in SD medium supplemented with leucine, isoleucine, valine, and inositol at 30°C to an optical density at 600 nm of ca. 1. Five milliliters of 100% (wt/vol) trichloroacetic acid was added to 20 ml of culture to minimize the proteolysis; the cultures were placed on ice with occasional shaking for 5 min. The cells were collected by centrifugation at 4,000 × *g* and broken by vortexing with glass beads for 2 min in 400 μl of lysis buffer (20 mM Tris-HCl [pH 7.5], 100 mM KCl, 30 mM $MgSO_4$, 1 mM dithiothreitol) as described previously (8). The lysates were cleared by centrifugation at 10,000 × *g* and neutralized by addition of 1/4 volume of 1 M Tris-HCl (pH 9.0). The protein concentrations in the extracts were determined by the Bradford method (1), using a dye reagent purchased from Bio-Rad and bovine serum albumin as the standard. Fifty micrograms of each extract was fractionated by sodium dodecyl sulfate (SDS)-polyacrylamide gel electrophoresis (PAGE) (10% gel), transferred to a nitrocellulose filter, and probed with antibodies as described in the legend to Fig. 2.

Isoelectric focusing PAGE analysis of eIF2α phosphorylation. Strain H1608 transformed with high-copy-number plasmids encoding different eIF2B subunits were grown for 7 h in liquid SD medium supplemented with leucine and inositol. Total protein extracts were prepared and subjected to isoelectric focusing slab gel electrophoresis exactly as described previously (10) and then subjected to immunoblot analysis using antibodies against eIF2α and an ECL (enhanced chemiluminescence) detection kit (Amersham) as instructed by the vendor.

Expression of TrpE-GCD2 fusion protein and affinity purification of GCD2 antibodies. The insoluble form of the TrpE-GCD2 fusion protein encoded by p2234 was isolated from *E. coli* RR1 as described elsewhere (24). Seven hundred micrograms of protein extract was separated by SDS-PAGE, using an 8-cm-wide 10% gel, and transferred to a nitrocellulose membrane. Antibodies directed against GCD2 residues 136 to 288 were purified from 250 μl of crude GCD2-specific antiserum (26), using a 1-cm^2 nitrocellulose membrane containing ca. 180 μg of the TrpE-GCD2 fusion protein, as described elsewhere (12).

Coimmunoprecipitation analysis of overexpressed eIF2B subunits. One-hundred-milliliter cultures of yeast strains carrying different high-copy-number plasmid(s) were grown in SD medium containing supplements described in the figure legends to an optical density at 600 nm of ca. 1.0. Cells were harvested, resuspended in 750 μl of lysis buffer (20 mM Tris-HCl [pH 7.5], 100 mM KCl, 30 mM $MgSO_4$, 1 mM dithiothreitol) containing protease inhibitors (1 mM phenylmethylsulfonyl fluoride, pepstatin A [0.7 μg/ml], leupeptin [1 μg/ml], and aprotinin [1 μg/ml]) as described previously (8), and disrupted by three 40-s bursts with 1-min intervals between each burst in a Braun homogenizer (8). The whole-cell extracts were cleared by centrifugation at 22,000 × *g* for 10 min. For coimmunoprecipitations, 0.1 g of protein A–Sepharose CL-4B beads (Pharmacia) was swollen in 100 mM *N*-2-hydroxyethylpiperazine-*N*′-2-ethanesulfonic acid (HEPES; pH 7.5) containing 1 mg of bovine serum albumin per ml. The beads were washed three times with 2 ml of binding buffer (20 mM Tris-HCl [pH 7.5], 50 mM KCl, 0.1% Triton X-100) and resuspended in 2 ml of binding buffer. Twenty micrograms of affinity-purified GCD2 antibody specific for GCD2 residues 136 to 288 or 20 μg of monoclonal antibody 12CA5 against the HA epitope (Boehringer Mannheim) was incubated with 40 μl of protein A-Sepharose beads (Pharmacia) in 200 μl of binding buffer for 1 h at room temperature with rocking. The beads were collected by centrifugation for 5 s and washed twice with 500 μl of binding buffer. Whole-cell extracts were added to 40 μl of beads that had been prebound with antibodies, and the total volume of the sample was brought to 200 μl with Co-IP buffer (20 mM Tris-HCl [pH 7.5], 75 mM KCl, 15 mM $MgSO_4$, 1 mM dithiothreitol, 0.05% Triton X-100) containing protease inhibitors as described above. The mixtures were incubated at 4°C for 2 h with rocking, and the beads were allowed to sediment by gravity for 10 min and then subjected to three washes, each time using 500 μl of Co-IP buffer, rocking for 1 min, and collecting the beads by centrifugation in a CAPSULE HF-120 microcentrifuge (Tomy Seiko Co.) for 5 s. Whole-cell extracts, pellet, and supernatant fractions were subjected to SDS-PAGE (10% gel), blotted to a nitrocellulose membrane (Novex Inc., San Diego, Calif.), and probed with antibodies against the yeast eIF2B and eIF2α subunits as described previously (4, 8, 11). The immunoblots were developed with ^{125}I-labeled protein A (2) or by using an ECL kit from Amersham as instructed by the vendor.

RESULTS

Overexpression of GCD2, GCD7, and GCN3 reduced the inhibitory effect of eIF2 phosphorylation on cell growth. To determine whether overexpressing individual subunits of eIF2B, or different combinations of the subunits, would rescue the native eIF2B complex from the inhibitory effects of phosphorylated eIF2, we constructed high-copy-number plasmids encoding one or more subunits of eIF2B and introduced them into a yeast strain (H1608) containing the constitutively activated protein kinase encoded by the *GCN2^c-M719V*, *E1537G* allele. This strain exhibits a severe slow-growth phenotype that can be attributed to a general inhibition of translation initiation in response to high-level phosphorylation of eIF2 (28). In accordance with our previous results (11), introducing the genes encoding all five subunits of eIF2B, or all four essential subunits of eIF2B (excluding *GCN3*), on high-copy-number plasmids into strain H1608 greatly decreased the toxic effects of the *GCN2^c* allele on cell growth (Table 1). All five subunits were found to be comparably overexpressed in these two types of transformants at a steady-state level ca. fivefold-greater than the wild-type level (11). We found that increasing the gene dosage for each of the subunits individually had no significant effect on the growth rate of H1608; however, three novel combinations of multicopy genes that partially suppressed the growth-inhibitory effects of the *GCN2^c* allele were identified: *GCD2*, *GCD7*, *GCD6*, and *GCN3*; *GCD2*, *GCD7*, and *GCN3*; and *GCD2* and *GCD7* (Table 1 and Fig. 1). Various other combinations of eIF2B subunit genes were tested and found to confer no significant growth stimulation in H1608 (Table 1 and Fig. 1). Two of the three novel suppressing gene combinations have *GCD2*, *GCD7*, and *GCN3* in common, and all three have *GCD2* and *GCD7*. These findings suggested that GCD2, GCD7, and GCN3 might form an eIF2B subcomplex that can interact with phosphorylated eIF2 and prevent it from inhibiting the native eIF2B complex. The suppressor activity of the combination of high-copy-number *GCD2* and *GCD7* could indicate that these proteins form a heterodimer that also can interact with eIF2(αP); alternatively, they might titrate GCN3 from the native eIF2B complex, leaving the four-subunit form of eIF2B that is less sensitive to eIF2(αP).

TABLE 1. Effects of overexpression of eIF2B subunits on cellular growth rate in a yeast strain containing an activated GCN2^c kinase[a]

Plasmid(s)	Overexpressed eIF2B subunit(s)	Relative growth rate[b]
pRS426	None	6+[c]
pRS426	None	1+
p1871	GCD2, GCD7, GCN3	3+
p1872	GCD2, GCD7	3+
p2299	GCD2, GCN3	1+
p2298	GCD7, GCN3	1+
p2297	GCD2	1+
p2305	GCD7	1+
p2304	GCN3	1+
p2301	GCD1	1+
p2300	GCD6	1+
p2302	GCD1, GCD6	1+
p2303	GCD1, GCD6, GCD2	1+
p1873, p2299	GCD1, GCD6, GCD2, GCN3	1+
p1871, pJB115	GCD2, GCD7, GCN3, GCD6	3+
p1873, p1872	GCD1, GCD6, GCD2, GCD7	5+
p1873, p1871	GCD1, GCD6, GCD2, GCD7, GCN3	4+

[a] Strain H1608 containing *GCN2^c-M719V, E1537G* was transformed with high-copy-number plasmids encoding the indicated eIF2B subunits or with empty vector pRS426, and the relative growth rates of the transformants were determined by examining colony size as described for Fig. 1.

[b] 6+, 5+, 4+, 3+, and 1+ designate colony sizes of ca. 1.5, 1.3, 1.1, 0.8, and 0.2 mm in diameter, respectively.

[c] Relative growth rate of the isogenic wild-type *GCN2* strain H1402 examined as a control.

Using immunoblot analysis, we verified that GCD2, GCD7, and GCN3 were comparably overexpressed in various transformants bearing combinations of only these three genes on high-copy-number plasmids. As expected, GCD1 and GCD6 were produced at wild-type levels in these particular strains (Fig. 2; compare lanes 1 to 5). Thus, the fact that introducing plasmids containing only *GCD2* and *GCN3*, or only *GCD7* and *GCN3*, did not suppress the toxic effects of eIF2 phosphorylation cannot be explained by the failure to overproduce the relevant proteins. Similarly, GCD1 and GCD6 were comparably overproduced in the transformant bearing only the genes encoding these two subunits in high copy number (Fig. 2, lane 8), indicating that GCD1 and GCD6 cannot form a complex that neutralizes the toxicity of a *GCN2^c* allele. By probing different amounts of the protein extracts, we estimated that GCD2, GCD7, and GCN3 were each overproduced ca. sevenfold in the strain containing all three genes on high-copy-number plasmids (see Fig. 7A).

An alternative explanation for our results could be proposed in which overexpressing GCD2 and GCD7, or GCD2, GCD7, and GCN3, would increase the level of the four- or five-subunit functional eIF2B complexes rather than producing a subcomplex that neutralizes eIF2(αP). In one variation of this model, GCD1 and GCD6 would normally be synthesized in higher molar amounts than the other three subunits, and when GCD2, GCD7, and GCN3 were overproduced, the excess GCD1 and GCD6 would be utilized to form greater amounts of five-subunit eIF2B instead of being turned over. This possibility was eliminated by the results in Fig. 2 showing that overproduction of GCD2, GCD7, and GCN3 did not lead to a detectable increase in the steady-state amounts of GCD1 and GCD6. In a second variation, GCD1 and GCD6 would be overproduced relative to the other subunits in wild-type cells, but the excess proteins not incorporated into eIF2B would be stable in the cytoplasm. In this case, we would not expect to see an increase in GCD1 and GCD6 protein levels when GCD2, GCD7, and GCN3 were overproduced (as shown in Fig. 2) and more five-subunit eIF2B was formed from the putative pools of monomeric GCD1 and GCD6. One argument against this possibility comes from the fact that the majority of all five subunits of eIF2B can be coimmunoprecipitated from wild-type cells by using antibodies specific for GCD6 (4, 8), GCD2 (8), or GCD1 (7). These previous results are inconsistent with the idea that GCD1 and GCD6 are normally produced in excess of the other subunits and exist independently of five-subunit eIF2B. In addition, if overexpression of GCD2, GCD7 and GCN3 led to higher levels of five-subunit eIF2B, there should have been increased amounts of GCD1 and GCD6 coimmunoprecipitating with GCD2, GCD7, and GCN3 in strains overexpressing only the latter three proteins. As shown below (Fig. 5A), this was not the case.

A third alternative explanation for our findings is that GCD2, GCD7, and GCN3 can form a trimeric subcomplex that catalyzes guanine nucleotide exchange on eIF2. Thus, overproducing these three proteins alone would increase the level of eIF2B recycling activity without increasing the concentration of five-subunit eIF2B. Genetic data inconsistent with this possibility are that deletions of *GCD1* (16) or *GCD6* (3) are lethal, and numerous conditional lethal mutations in *GCD1* and *GCD6* increase *GCN4* expression at the permissive temperature, indicative of a reduction in eIF2 recycling. The *gcd6-1* mutation is lethal at 36°C and, as shown in Fig. 3A, leads to a slow-growth phenotype (Slg$^-$) at 30°C (3). It could be proposed that GCD6 is not essential for catalytic activity and the *gcd6-1* mutation reduces eIF2B function primarily by destabilizing the complex and decreasing the steady-state levels of the

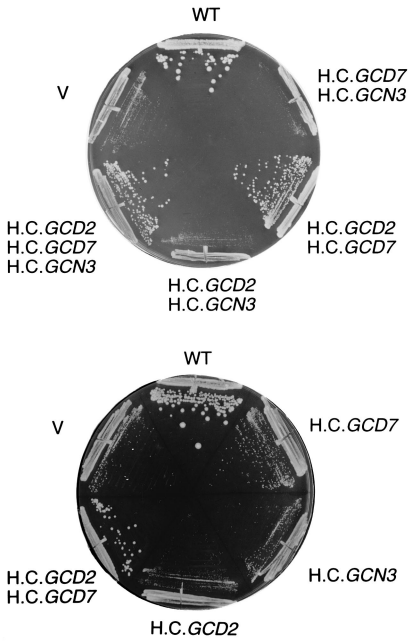

FIG. 1. Cooverexpression of GCD2, GCD7, and GCN3 or just GCD2 and GCD7 alleviates the slow-growth phenotype associated with a constitutively activated form of protein kinase GCN2. Strain H1608 bearing the chromosomal *GCN2^c-M719V, E1537G* allele was transformed with high-copy-number (H.C.) plasmids encoding the indicated eIF2B subunit gene(s) or with empty vector (V). Isogenic *GCN2* strain H1402 was transformed with empty vector to provide a wild-type control (WT). The transformants were streaked on minimal SD medium supplemented with leucine, isoleucine, valine, and inositol and incubated at 30°C for 3 days. The high-copy-number plasmids were p1871 (*GCD2*, *GCD7*, *GCN3*), p2297 (*GCD2*), p1872 (*GCD2*, *GCD7*), p2298 (*GCD7*, *GCN3*), p2299 (*GCD2*, *GCN3*), p2304 (*GCN3*), p2305 (*GCD7*), and pRS426 (V).

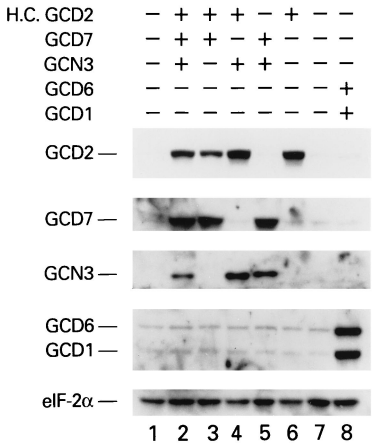

FIG. 2. Immunoblot analysis of overexpressed eIF2B subunits. Strain H1402 bearing high-copy-number (H.C.) plasmids containing the genes indicated at the top (by + or −) were grown in liquid SD medium supplemented with leucine, isoleucine, valine, and inositol, and whole-cell extracts were prepared. Fifty micrograms of protein from each extract was fractionated by SDS-PAGE (10% gel) and transferred to a nitrocellulose membrane. Two identical filters were prepared, and each was cut in half at the position corresponding to 50 kDa. The top half of one filter was probed with antibodies specific for GCD6 (at 1:1,000 dilution) and GCD1 (at 1:200 dilution), and the bottom half was probed with antibodies against GCN3 (at 1:50 dilution). The top half of the second filter was probed with antibodies against GCD2 (at 1:1,000 dilution), and the bottom half was probed with antibodies against GCD7 (at 1:250 dilution) and eIF2α (at 1:1,000 dilution). The proteins detected with the different antisera are indicated to the left of the corresponding panels.

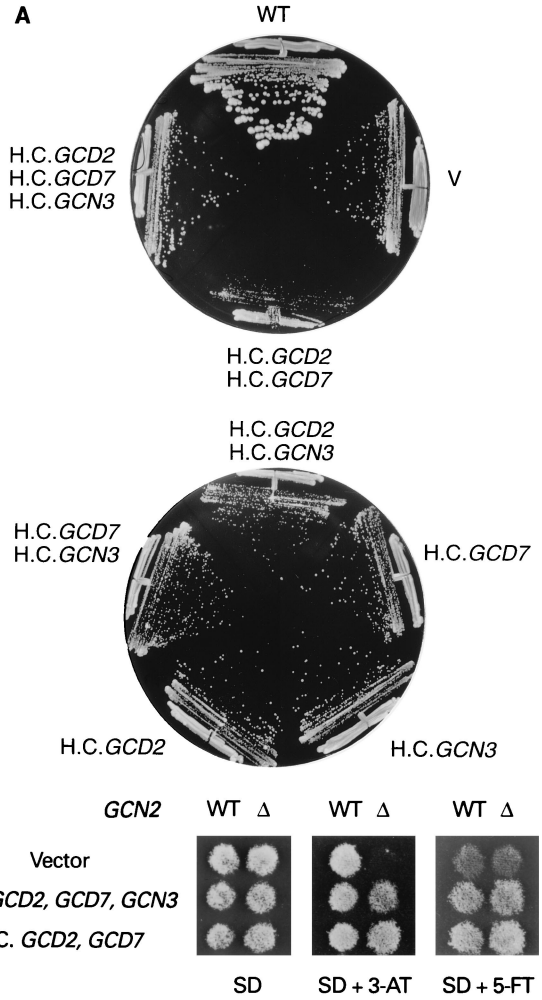

FIG. 3. Genetic evidence that overexpression of GCD2, GCD7, and GCN3 or just GCD7 and GCN3 does not increase recycling of eIF2. (A) Effect of overexpression of eIF2B subunits on the growth rate of *gcd6-1* strain H1728. H1728 was transformed with the following high-copy-number (H.C.) plasmids encoding eIF2B subunits: p1871 (*GCD2*, *GCD7*, *GCN3*), p1872 (*GCD2*, *GCD7*), p2298 (*GCD7*, *GCN3*), p2299 (*GCD2*, *GCN3*), p2297 (*GCD2*), p2304 (*GCN3*), and p2305 (*GCD7*). The transformants were streaked on SD medium supplemented with isoleucine, leucine, valine, and inositol and incubated at 30°C for 4 days. WT, H1728 transformed with plasmid p2300 containing *GCD6* to show the wild-type growth rate; V, H1728 transformed with empty vector pRS426 to show the slow-growth phenotype of *gcd6-1*. (B) Isogenic *GCN2* (WT) and *gcn2*Δ (Δ) strains transformed with high-copy-number plasmid p1871 (row 2) or p1872 (row 3), carrying the indicated eIF2B subunit genes, or with empty vector pRS426 (row 1) were grown to confluence on SD medium supplemented with leucine, isoleucine, valine, and inositol and replica plated on the same medium (SD) or on medium supplemented with 10 mM 3-AT (SD + 3-AT) or 0.5 mM 5-FT (SD + 5-FT). The 3-AT and 5-FT plates were incubated for 3 days at 30°C; the SD plate was incubated for 1 day at 30°C.

GCD2, GCD7, and GCN3 subunits which would comprise the catalytic domain. If this were true, then the high-copy-number plasmids encoding these three proteins might provide sufficient levels of recycling activity to suppress the Slg$^-$ phenotype of the *gcd6-1* mutant. As shown in Fig. 3A, this was not the case. Thus, whereas overexpressing GCD2, GCD7, and GCN3 reduced the toxic effects of eIF2 phosphorylation on eIF2B function (Table 1 and Fig. 1), it did not compensate for the reduction in activity caused by a mutation in a different subunit of eIF2B.

An additional argument against the idea that GCD2, GCD7, and GCN3 can recycle eIF2 independently of the other subunits of eIF2B is that overexpressing these three subunits in a strain lacking GCN2 actually appeared to decrease, rather than increase, eIF2 recycling. Mutants lacking GCN2 are unable to derepress *GCN4* translation and amino acid biosynthetic genes under GCN4 control in response to amino acid starvation; consequently, they cannot grow on medium containing 3-AT, an inhibitor of histidine biosynthesis. The inability to derepress *GCN4* translation and the attendant 3-AT sensitivity in *gcn2*Δ mutants are suppressed by recessive mutations in subunits of eIF2B that are thought to decrease eIF2 recycling independently of eIF2(αP). Because they constitutively derepress amino acid biosynthetic genes under GCN4 control, *gcd* mutations also confer increased resistance to the tryptophan analog 5-FT in both *GCN2* and *gcn2*Δ backgrounds. We found that overexpressing GCD2, GCD7, and GCN3, or just GCD2 and GCD7, partially suppressed the 3-AT-sensitive phenotype of a *gcn2*Δ strain and led to 5-FT resistance in both *GCN2* and *gcn2*Δ strains (Fig. 3B). Because these phenotypes are hallmarks of loss-of-function mutations in eIF2B, we conclude that overexpressing GCD2, GCD7, and GCN3 or just GCD2 and GCD7 leads to a modest decrease in recycling of eIF2 in *gcn2*Δ strains and in *GCN2* cells under nonstarvation conditions. This probably occurs by the formation of defective incomplete complexes containing GCD2, GCD7, and GCD6 (lacking GCD1) or containing GCD2, GCD7, and GCD1 (lacking GCD6).

It was conceivable that overexpressed GCD2, GCD7, and GCN3 formed a complex that interacted with eIF2 in a way that reduced phosphorylation of the α subunit by GCN2. To eliminate this possibility, we used isoelectric focusing PAGE to measure the ratios of phosphorylated to nonphosphorylated eIF2α in *GCN2^c* strains overexpressing different eIF2B subunits. As shown in Fig. 4 (lane 4), ca. 50% of the eIF2α was phosphorylated in the strain transformed with vector alone and in strains overexpressing GCD2 (lane 3), GCD2 and GCN3

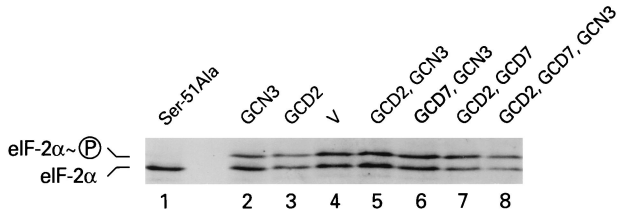

FIG. 4. Analysis of eIF2α phosphorylation in the *GCN2*^{c}*-M719V*, *E1537G* strain overexpressing eIF2B subunits. Strain H1608 was transformed with high-copy-number plasmids encoding the indicated eIF2B subunits and grown under nonstarvation conditions in liquid SD supplemented with leucine, isoleucine, valine, and inositol. Total-protein extracts were prepared and subjected to isoelectric focusing PAGE followed by immunoblot analysis using antibodies against eIF2α. The hyperphosphorylated form of eIF2α migrated above the basally phosphorylated species (eIF2α). An extract from strain H2429 (35) expressing eIF2α containing Ala in place of Ser at position 51 was included to show the position of basally phosphorylated eIF2α (lane 1). The following high-copy-number plasmids were present in the transformants: p2304, (*GCN3*; lane 2), p2297 (*GCD2*; lane 3), pRS426 (vector [V]; lane 4); p2299 (*GCD2*, *GCN3*; lane 5); p2298 (*GCD7*, *GCN3*; lane 6); p1872 (*GCD2*, *GCD7*; lane 7), and p1871 (*GCD2*, *GCD7*, *GCN3*; lane 8).

(lane 5), and GCD7 and GCN3 (lane 6). In the strains overexpressing GCD2 and GCD7 (lane 7) or GCD2, GCD7, and GCN3 (lane 8), the proportion of phosphorylated eIF2 was increased slightly, eliminating the possibility that overexpressing these combinations of subunits decreases eIF2 phosphorylation. An increase in eIF2α phosphorylation has also been observed in strains bearing *GCD7* or *GCD2* mutations that overcome eIF2(αP) toxicity (9, 27, 35).

Biochemical evidence for the formation of an eIF2B subcomplex containing GCD2, GCD7, and GCN3. We next sought biochemical evidence that the excess GCD2, GCD7, and GCN3 produced in cells overexpressing these three proteins formed an eIF2B subcomplex. Toward this end, we immunoprecipitated whole-cell extracts with affinity-purified antibodies against GCD2 and probed the immune complexes and supernatants with antibodies against each of the eIF2B subunits. As shown in Fig. 5A (lane 4), the GCD2-specific antibodies immunoprecipitated the majority of the GCD2 and GCD7 and ca. 50% of the GCN3 present in the extract. If the excess GCD7 and GCN3 were not complexed with GCD2, then antibodies against GCD2 should have immunoprecipitated only the amounts of GCD7 and GCN3 present in the five-subunit form of eIF2B, which are barely visible in the pellet fractions obtained from wild-type extracts (Fig. 5A, lane 3). Instead, the GCD2 antibodies immunoprecipitated GCD7 and GCN3 from the strain overexpressing all three proteins (lane 4) far in excess of the amounts coimmunoprecipitated with GCD2 from the wild-type strain. These are the results expected if the excess GCD2, GCD7, and GCN3 coexist in the same subcomplexes. The interaction between GCD2 and GCD7 in the subcomplex was found to be stable in buffers containing between 75 and 400 mM KCl (data not shown). In a control experiment, antibodies against GCD6 were used to immunoprecipitate eIF2B from these extracts, and as expected, all five subunits of eIF2B were coimmunoprecipitated with GCD6. Importantly, essentially the same amounts of GCD2, GCD7, and GCN3 were coimmunoprecipitated with GCD6 from the extracts containing overexpressed amounts of these three proteins or from wild-type extracts (data not shown). These results indicate that the bulk of the overexpressed GCD2, GCD7, and GCN3 proteins are present in complexes that do not contain GCD6.

To confirm the results of the preceding experiments, we carried out a similar coimmunoprecipitation analysis using a strain which overexpresses a mutant GCD2 protein lacking

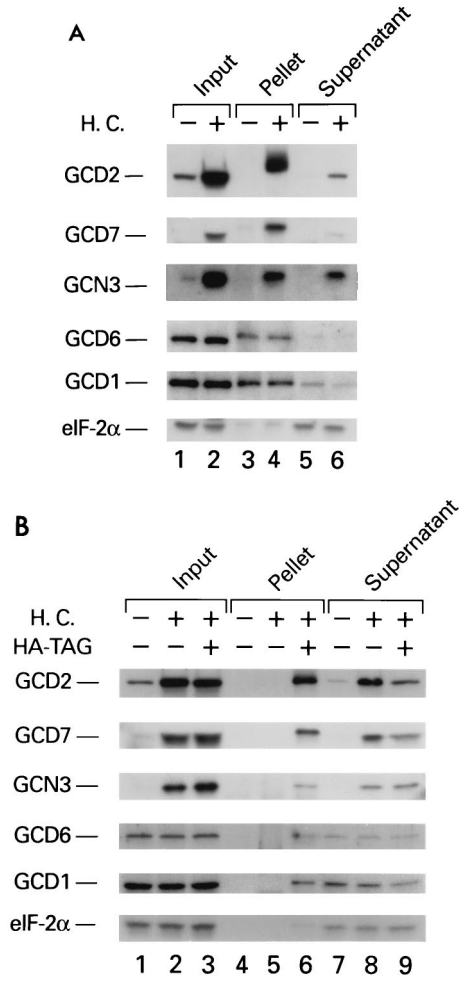

FIG. 5. Coimmunoprecipitation of overexpressed GCD2, GCD7, and GCN3. Transformants of strain BJ1995 bearing high-copy-number plasmids for overexpressing GCD2, GCD7, and GCN3 or control plasmids were grown in liquid SD medium supplemented with tryptophan and leucine (A) or only tryptophan (B), and whole-cell extracts were prepared. Immunoprecipitations were performed either with affinity-purified antibodies against GCD2 that recognize residues 136 to 288 in the N-terminal region of the protein (A) or with monoclonal antibodies against the HA epitope (B). Fifty micrograms of whole-cell extract (Input), the immune complexes isolated from 50 μg of extract (Pellet), and the supernatant fractions corresponding to 25 μg of starting extract (Supernatant) were subjected to SDS-PAGE (10% gel) and immunoblot analysis as described in Materials and Methods and the legend to Fig. 2. The antisera used in the immunoblot analysis are shown to the left of each panel. (A) H.C.: +, transformant bearing high-copy-number plasmid p1871 containing *GCD2*, *GCD7*, and *GCN3* (lanes 2, 4, and 6); −, transformant bearing empty vector pRS426 (lanes 1, 3, and 5). We routinely observed a decrease in mobility of the proteins in the pellet fractions versus the input fractions, which we attribute to the high levels of immunoglobulin G present in the pellet fractions. GCD2 shows an additional decrease in mobility which may reflect a covalent modification of the protein during the immunoprecipitations. We found that the N-terminal 30% of GCD2 was required to observe this alteration (data not shown). (B) H.C.: +, transformant bearing high-copy-number plasmids p2298 and p1874 (lanes 2, 5, and 8) containing *GCD7*, *GCN3*, and *GCD2* (lacking the HA epitope) or p2298 and p1876 (lanes 3, 6, and 9) containing *GCD7*, *GCN3*, and *HA-GCD2*(*Δ4-26*); −, transformant bearing empty vectors pRS425 and pRS426 (lanes 1, 4, and 7). HA-TAG: −, transformant expressing untagged GCD2; +, transformant expressing HA-tagged GCD2. In panel B, the amounts of several of the proteins in the pellet and supernatant fractions did not add up to the input amounts in the starting extract. This could be attributed to losses from the pellet fractions during the washing steps or to degradation during the immunoprecipitations. We favor the former because this phenomenon was not observed using antibodies against GCD2; in addition, the efficiency of immunoprecipitation of HA-tagged GCD2 with anti-HA antibodies was less efficient than with anti-GCD2 antibodies, suggesting that the immune complexes obtained with anti-HA antibodies are less tightly bound to the protein A beads.

amino acids 4 to 26 and containing the HA epitope tag at the N terminus. The *HA-GCD2*(Δ*4-26*) and wild-type *GCD2* alleles were indistinguishable in their ability to complement a *gcd2*Δ mutation and to suppress the slow-growth phenotype of *GCN2*^{c} strains when overexpressed with GCD7 and GCN3 (data not shown). In addition, the HA-tagged and untagged forms of GCD2 accumulated to similar levels when cooverexpressed with GCD7 and GCN3 (Fig. 5B, lanes 2 and 3). We used monoclonal antibodies against the HA epitope to immunoprecipitate HA-GCD2(Δ4-26) and probed the pellet and supernatant fractions with antibodies against GCD2 and each of the other four subunits of eIF2B. Comparison of the pellet and supernatant fractions in lanes 6 and 9 of Fig. 5B indicates that the majority of the overexpressed HA-tagged GCD2 and GCD7 were coimmunoprecipitated by HA antibodies, confirming that most of the excess amounts of these proteins were complexed with one another in the overproducing strain. Compared with what was seen for GCD7, a significantly smaller fraction of GCN3 was coimmunoprecipitated with HA-tagged GCD2; nevertheless, this amount of GCN3 was substantially greater than the wild-type complement of GCN3 visible in control extracts (compare signals for GCN3 in lanes 6 and 1 in Fig. 5B). Thus, a significant fraction of the excess GCN3 was also complexed with the HA-tagged form of GCD2 in the overproducing strain. It is possible that the HA tag on GCD2 decreases the stability of the GCD2-GCD7-GCN3 subcomplex, leading to dissociation of an even larger fraction of GCN3 from the subcomplex during the washing steps of the immunoprecipitations than was seen with untagged GCD2 (Fig. 5A).

In the experiment shown in Fig. 5A, we also probed the immunoprecipitates for the α subunit of eIF2 to examine the possibility that the GCD2-GCD7-GCN3 subcomplex can stably interact with eIF2. In agreement with previous findings, only a small fraction of eIF2α coimmunoprecipitated with GCD2 from the wild-type control extracts (Fig. 5A, lanes 3 and 5), reflecting the fact that eIF2 is present in large molar excess over eIF2B and that most of the eIF2 does not copurify with eIF2B (8). The same proportion of eIF2α was immunoprecipitated with GCD2 antibodies from the extract containing overexpressed GCD2, GCD7, and GCN3 as from the control wild-type extracts (Fig. 5A, lanes 3 to 6). Thus, either eIF2 cannot bind to the subcomplex containing GCD2, GCD7, and GCN3 or, as we suggest below, the interaction between the subcomplex and eIF2 is too unstable or short-lived to detect in coimmunoprecipitation experiments.

Evidence that cooverexpression of GCD2 and GCD7 titrates the GCN3 subunit from eIF2B. The fact that overexpressing only GCD2 and GCD7 suppresses the slow-growth phenotype of the *GCN2*^{c} allele (Fig. 1) could indicate that these two proteins form a heterodimer that is capable of competing with native eIF2B for interaction with eIF2(αP), in the same manner proposed above for the GCD2-GCD7-GCN3 subcomplex. This possibility was consistent with results from the coimmunoprecipitation experiments in Fig. 5, in which a greater fraction of GCD7 than of GCN3 was coimmunoprecipitated with GCD2 from strains overproducing all three proteins. When we examined coimmunoprecipitation of GCD7 with GCD2 from strains overexpressing only these two proteins, however, we found only a small fraction of the excess GCD7 coimmunoprecipitating with GCD2 (data not shown). These results indicate that either a GCD2-GCD7 binary complex does not form at high levels in vivo or it is less stable than the GCD2-GCD7-GCN3 trimeric complex and dissociates in the course of the coimmunoprecipitations.

If GCD2 and GCD7 formed a binary complex that competes with eIF2B for binding eIF2(αP), then overexpressing GCD2 and GCD7 should suppress the toxicity of eIF2(αP) even in strains lacking *GCN3*. We could not test this prediction in the *GCN2*^{c}*-M719V*, *E1537G* strain because deletion of *GCN3* is sufficient to suppress the slow-growth phenotype of this allele (28). Therefore, we examined whether overexpressing GCD2 and GCD7 would reduce the toxicity of expressing the human eIF2(αP) kinase PKR in a *gcn3*Δ strain. As shown previously (9), high-level expression of PKR in a wild-type strain was lethal, whereas PKR expression in an isogenic *gcn3*Δ mutant conferred a slow-growth phenotype (Fig. 6A). Thus, the four-subunit form of eIF2B lacking GCN3 is less sensitive than wild-type eIF2B but is still susceptible to high levels of eIF2(αP) produced in yeast cells expressing PKR. Overexpression of GCD2 and GCD7 in the *gcn3*Δ strain did not reduce the toxicity of PKR expression and in fact exacerbated the

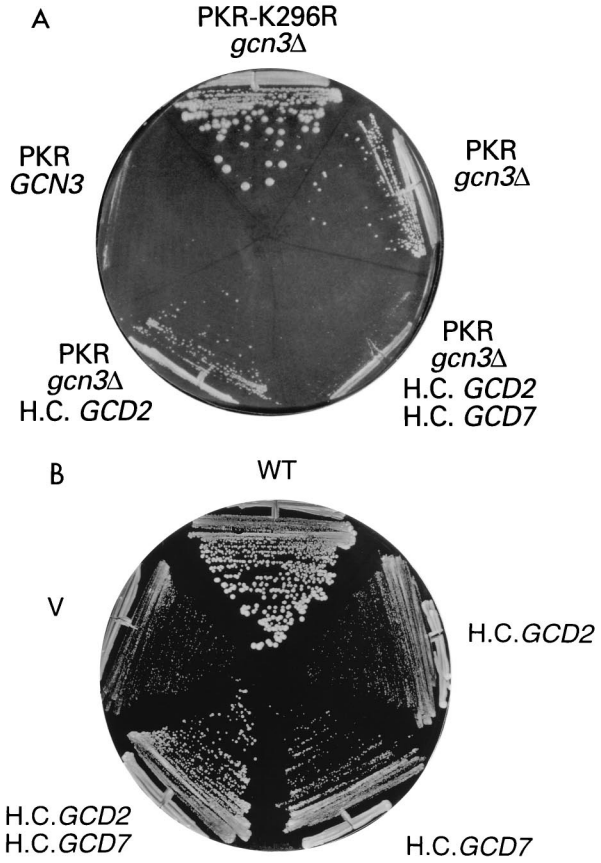

FIG. 6. Genetic evidence that overexpression of GCD2 and GCD7 suppresses the toxicity of eIF2(αP) by stripping GCN3 from eIF2B. (A) Overexpression of GCD2 and GCD7 does not suppress the toxicity of the human eIF2(αP) kinase PKR in a *gcn3*Δ strain. The *gcn3*Δ strain GP3153 was transformed with plasmid p1545 containing the cDNA encoding human PKR under the control of a galactose-inducible promoter, or a derivative of this plasmid encoding the catalytically defective mutant kinase PKR-K296R (p1421), and with a high-copy-number (H.C.) plasmid bearing *GCD2* (p2297), *GCD2* and *GCD7* (p1872) or no insert (pRS426). In addition, GP3153 was transformed with p2304 containing *GCN3* and with the empty vector pRS424A. A transformant of each strain was streaked on minimal medium containing 10% galactose as the carbon source and incubated for 9 days at 30°C. (B) Overexpression of GCD2 and GCD7 alleviates the slow-growth phenotype of *gcn3*^{c}*-R104K*. Strain H1489 bearing the chromosomal *gcn3*^{c}*-R104K* allele was transformed with high-copy-number plasmids bearing the indicated genes (p2297, *GCD2*; p2305, *GCD7*; p1872, *GCD2* and *GCD7*) or with empty vector (V; pRS426). Transformants were streaked on SD plates containing leucine, isoleucine, valine, and inositol and incubated at 30°C for 2 days. WT, isogenic wild-type strain H1402 transformed with empty vector pRS426.

growth defect associated with eIF2 hyperphosphorylation (Fig. 6A). These results are inconsistent with the idea that overexpressing GCD2 and GCD7 suppresses the toxicity of eIF2 phosphorylation by forming a heterodimer that competes with eIF2B for binding eIF2(αP). The fact that overexpressing GCD2 and GCD7 in the *gcn3*Δ strain exacerbated the toxicity of PKR expression is in accordance with results described above (Fig. 3) indicating that eIF2B function is reduced when GCD2 and GCD7 are cooverexpressed, presumably because eIF2B is partially dissociated into nonfunctional subcomplexes.

The alternative hypothesis to explain the suppressor activity of overexpressing GCD2 and GCD7 is that these proteins can titrate GCN3 from five-subunit eIF2B into the three-subunit GCD2-GCD7-GCN3 subcomplex, leaving the four-subunit eIF2B complex that is less sensitive to eIF2(αP) (9, 14). We reasoned that if this hypothesis was correct, then overexpression of GCD2 and GCD7 should suppress the slow-growth phenotype associated with a *GCN3* mutation that impairs eIF2B catalytic activity. The *gcn3^c-R104K* allele leads to slow growth on rich medium (Fig. 6B) and 3-AT resistance in a *gcn2*Δ strain (14), characteristic of loss-of-function *gcd* mutations in essential subunits of eIF2B (17). Thus, it appears that the *gcn3^c-R104K* mutation interferes with the function of eIF2B even though a complete deletion of *GCN3* does not. We found that cooverexpression of GCD2 and GCD7 partially suppressed the slow-growth phenotype of the *gcn3^c-R104K* strain, whereas overexpression of GCD2 or GCD7 alone had little (GCD7) or no (GCD2) effect on the growth rate of the *gcn3^c-R104K* strain (Fig. 6B). These results are consistent with the idea that cooverexpression of GCD2 and GCD7 leads to removal of a fraction of GCN3 (or in this case the *gcn3^c-R104K* product) from eIF2B and formation of the trimeric subcomplex. The weak suppression conferred by high-copy-number *GCD7* may indicate that excess GCD7 alone can titrate a fraction of GCN3 away from eIF2B. This would be consistent with the fact that GCD7 and GCN3 are the two most homologous subunits in eIF2B (3).

If cooverexpressing only GCD2 and GCD7 suppresses eIF2(αP) toxicity by titrating GCN3 from eIF2B, the same mechanism might operate when overexpressing all three proteins if GCD2 and GCD7 were overproduced to a greater extent than was GCN3. In this event, the excess GCD2 and GCD7 would titrate GCN3 from eIF2B and produce the four-subunit form of eIF2B. To eliminate this possibility, we examined the effect of increasing *GCN3* dosage further in a strain overexpressing all three proteins. This was accomplished by introducing a second high-copy-number plasmid bearing *GCN3* (p1999) into the strain containing the high-copy-number plasmid bearing *GCD7*, *GCD2*, and *GCN3* (p1871). Immunoblot analysis confirmed that GCN3 was overexpressed in the strain containing both p1999 and p1871 at ca. twofold-higher levels than in the strain bearing p1871 alone (Fig. 7A; compare the GCN3 signals in lanes 2 and 3 and lanes 5 and 6). If the *GCN2^c* allele was suppressed in the strain bearing p1871 as a result of titration of GCN3 from eIF2B by excess GCD2 and GCD7, then suppression should be abolished when the level of GCN3 is doubled by introduction of p1999 together with p1871. At odds with this prediction, we found that p1999 had no detectable effect on the ability of p1871 to suppress the *GCN2^c* allele (Fig. 7B). These results support our contention that overexpressing GCD2, GCD7, and GCN3 suppresses the *GCN2^c* allele by forming a trimeric subcomplex that protects native eIF2B from phosphorylated eIF2.

Evidence that the C-terminal half of GCD2 is sufficient for complex formation with GCD7 and GCN3. The regions of GCD2 that are similar in sequence to GCD7 and GCN3 are restricted to the C-terminal half of the protein. We have suggested that these three proteins directly interact with one another in the eIF2B complex and that these interactions are mediated by regions of sequence similarity among them (4, 20). In an effort to test this prediction, we progressively truncated HA-tagged GCD2 from the N terminus (Fig. 8A) and examined the phenotypes of overexpressing these N-terminal truncations alone or in combination with GCD7 and GCN3. Immunoblot analysis revealed that removal of residues 4 to 189 from the N terminus of HA-tagged GCD2 did not reduce the abundance of the protein relative to that of wild-type GCD2, whereas truncations to position 288 or 403 reduced steady-state amounts of the HA-tagged proteins to levels equal to (Δ4-288) or below (Δ4-403) that of wild-type GCD2 (Fig. 8B). Despite the low expression level for the Δ4-288 construct, it displayed a strong dominant-negative phenotype in strains overexpressing GCD7 and GCN3, as described next.

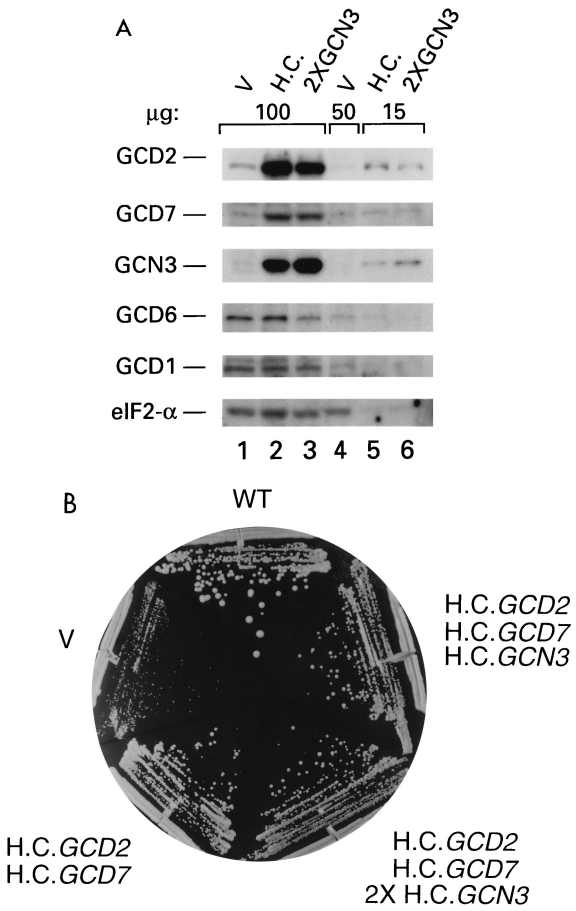

FIG. 7. Doubling the level of GCN3 does not alter suppression of the slow-growth phenotype of a *GCN2^c* allele by overexpressed GCD2, GCD7, and GCN3. Strain H1608 bearing *GCN2^c-M719V*, *E1537G* was transformed with high-copy-number plasmid p1871 (containing *GCD2*, *GCD7*, and *GCN3*) and empty vector pRS425 (H.C.; lanes 2 and 5), with p1871 plus p1999 (containing *GCN3*) (2XGCN3; lanes 3 and 6), or with empty vectors pRS425 and pRS426 (V; lanes 1 and 5). (A) Transformants were grown in liquid SD supplemented with isoleucine, valine, and inositol, and the indicated amounts of whole-cell extracts (100, 50, or 15 μg) were subjected to SDS-PAGE (10% gel) and immunoblot analysis using antibodies against the proteins listed to the left of each immunoblot, as described in the legend to Fig. 2. (B) The transformants of H1608 bearing the high-copy-number plasmids containing the indicated genes or empty vectors (V) were streaked on SD medium supplemented with isoleucine, valine, and inositol and grown at 30°C for 3 days. Isogenic *GCN2* strain H1402 transformed with empty vectors was streaked in parallel to provide a wild-type growth control (WT).

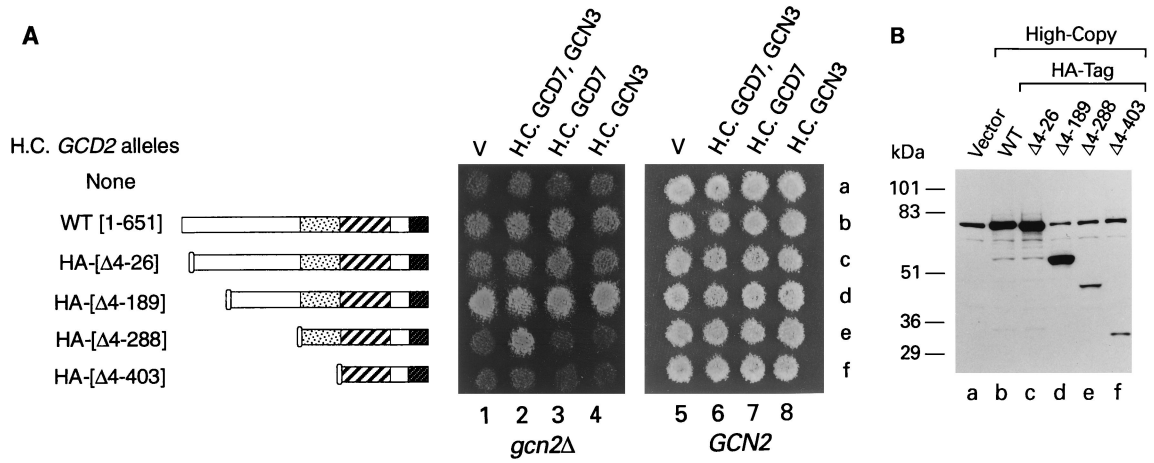

FIG. 8. Analysis of N-terminal truncations of GCD2. (A) Dominant-negative phenotype of the *HA-GCD2*(*Δ4-288*) allele requires overproduction of GCD7 and GCN3. Isogenic strains H2526 (*gcn2*Δ) and H1402 (*GCN2*) were transformed with high-copy-number (H.C.) plasmids carrying the *GCD2* alleles indicated on the left. The schematics depict the portion of GCD2 remaining in each allele, with shading used to indicate sequence similarity to GCD7 and GCN3. Strains also contained high-copy-number plasmids containing *GCD7* and/or *GCN3*, or empty vector, as indicated above the photographed results. The transformants were grown to confluence on SD plates supplemented with isoleucine, valine, and inositol and replica plated to the same medium supplemented with 10 mM 3-AT. The plasmid-borne *GCD2* alleles present in the various transformants were as follows: None, empty vector pRS425; WT (wild type) [1-651], p1874; HA-[Δ4-26], p1876; HA-[Δ4-189], p1875; HA-[Δ4-288], p1877; and HA-[Δ4-403], p1878. V (vector), pRS426; H.C. GCD7, GCN3, p2298; H.C. GCD7, p2305; H.C. GCN3, p2304. (B) Immunoblot analysis of N-terminally truncated GCD2 proteins expressed from high-copy-number plasmids. The transformants of strain H2526 analyzed in panel A containing *GCD7*, *GCN3*, and the indicated *GCD2* truncations on high-copy-number plasmids were grown in liquid SD supplemented with isoleucine, valine, and inositol, and whole-cell extracts were prepared. One hundred micrograms of protein was subjected to SDS-PAGE (10% gel) and immunoblot analysis using affinity-purified antibodies specific for the C terminus of GCD2 (residues 288 to 651) and ECL to visualize the immune complexes. Molecular size markers are shown on the left.

We began by examining the truncated HA-tagged GCD2 proteins when overexpressed with GCD7 and GCN3 for suppression of the slow-growth phenotype of the *GCN2*^{c} allele. Whereas the Δ4-26 truncation suppressed *GCN2*^{c}*-M719V*, *E1537G* indistinguishably from wild-type GCD2 when cooverexpressed with GCD7 or with GCD7 and GCN3, the more extensively truncated GCD2 proteins lacked this suppressor activity (data not shown). As shown in Fig. 8A, overexpressing HA-GCD2(Δ4-189) alone strongly suppressed the 3-AT-sensitive phenotype of the *gcn2*Δ allele, mimicking loss-of-function *gcd2* mutations, whereas wild-type GCD2 and the Δ4-29 truncation conferred only partial suppression (column 1, rows a to d). Neither of the more extensively truncated proteins lacking residues 4 to 288 or 4 to 403 suppressed the *gcn2*Δ allele when expressed alone (Fig. 8A, column 1, rows a, e, and f). These results suggested that the Δ4-189 truncated protein was functionally impaired but could be incorporated into eIF2B in place of wild-type GCD2, producing a defective form of the recycling factor. We verified that the *GCD2* alleles lacking residues 4 to 189, 4 to 288, and 4 to 403 were nonfunctional by showing that they could not rescue the lethality of a chromosomal deletion of *GCD2*; in contrast, strains containing wild-type *GCD2* or the *HA-GCD2*(*Δ4-26*) construct as the only *GCD2* allele had indistinguishable growth rates (see Materials and Methods).

With the exception of the Δ4-288 construct, the phenotypes of the *GCD2* truncations were not significantly altered from those just described when examined in the presence of either high-copy-number *GCD7* or *GCN3* (Fig. 8A, columns 2 to 4 and rows c, d, and f). In contrast, the Δ4-288 construct failed to suppress the 3-AT sensitivity of *gcn2*Δ in the strain overexpressing only GCD7 or GCN3 but strongly suppressed *gcn2*Δ when GCD7 and GCN3 were also being overexpressed (compare columns 1 to 4 in row e). To explain these last results, we suggest that the Δ4-288 protein alone cannot compete with wild-type GCD2 for incorporation into the eIF2B complex; however, it can interact with the excess GCD7 and GCN3 when these proteins are overproduced. The resulting trimeric complex can titrate a fraction of GCD1 or GCD6 into nonfunctional complexes, and the ensuing reduction in functional eIF2B leads to derepression of *GCN4* translation (3-AT resistance) in the absence of eIF2 phosphorylation in the *gcn2*Δ mutant.

If this interpretation is correct, we reasoned that it should be possible to coimmunoprecipitate a fraction of the GCD1 or GCD6 with the HA-GCD2(Δ4-288) truncated protein with HA antibodies from extracts from the strain cooverexpressing GCD7 and GCN3. Because this mutant protein does not accumulate to high levels, only a small fraction of the overproduced GCD7 and GCN3 would be expected to coimmunoprecipitate with it. In contrast, none of GCD7, GCN3, GCD1, or GCD6 should coimmunoprecipitate with this truncated GCD2 protein from extracts of the strain containing wild-type levels of GCD7 and GCN3. These expectations were borne out by the results shown in Fig. 9, showing that a small but significant fraction of GCD1 and GCD6, and a much smaller proportion of the excess amounts of GCD7 and GCN3, was coimmunoprecipitated with HA-GCD2(Δ4-288) from extracts of the strain overexpressing GCD7 and GCN3. These proteins were not coimmunoprecipitated with the truncated GCD2 protein from control extracts containing only wild-type levels of GCD7 and GCN3 (Fig. 9, lanes 6 and 7). We also observed that the steady-state level of the Δ4-288 protein in the extracts and the yield of this protein in the immunoprecipitations reproducibly increased ca. twofold when GCD7 and GCN3 were overexpressed (Fig. 9, lanes 3, 4, 6, and 7). In contrast with these results, the Δ4-189 protein was coimmunoprecipitated with a fraction of GCD1, GCD6, GCD7, and GCN3 in the absence of overexpressed GCD7 and GCN3 (Fig. 9, lanes 8 and 9). These data are in accordance with the finding that the Δ4-189 construct has a dominant-negative phenotype in the presence or absence of overexpressed GCD7 and GCN3 (Fig. 8A). The fact that the Δ4-288 protein can complex with a fraction of GCD1 and GCD6 (Fig. 9) and reduce eIF2B function (Fig. 8A) only

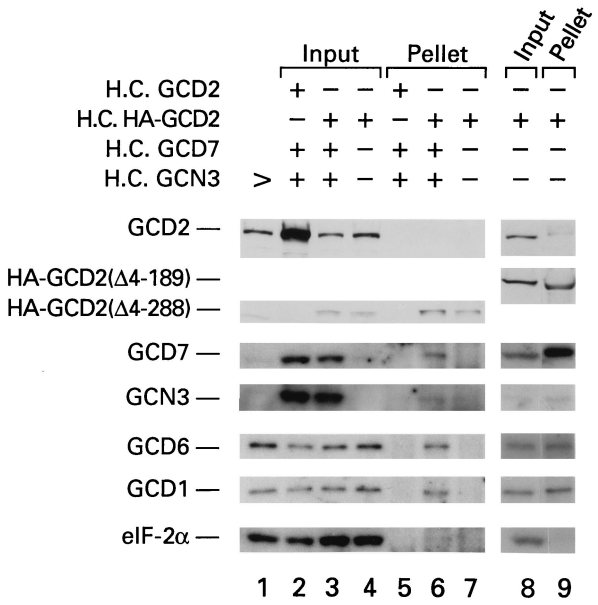

FIG. 9. Coimmunoprecipitation of N-terminally truncated GCD2 proteins with other eIF2B subunits. Whole-cell extracts were prepared from transformants of strain BJ1995 bearing high-copy-number (H.C.) plasmid p2298 containing *GCD7* and *GCN3*, or the corresponding empty vector pRS426, and also bearing p1874 (*GCD2*), p1875 (*GCD2-HA*-[*Δ4-189*]), or p1877 (*GCD2-HA*[*Δ4-288*]) containing the indicated *GCD2* alleles or the corresponding empty vector pRS425. Aliquots of extract containing 500 μg of protein were incubated with protein A beads prebound with monoclonal antibodies against the HA epitope, and the immune complexes were isolated and subjected to SDS-PAGE (10% gel) and immunoblot analysis using antibodies against the proteins listed to the left of each panel. The samples loaded in the lanes designated Input contained 83 μg of protein extract; those designated Pellet contained the immune complexes isolated from 500 μg of protein extract. High-copy-number plasmids present in the strains analyzed: lane 1, empty vectors pRS425 and pRS426; lanes 2 and 5, p2298 and p1874; lanes 3 and 6, p2298 and p1877; lanes 4 and 7, pRS426, p1877; lanes 8 and 9, pRS426 and p1875.

when GCD7 and GCN3 are overexpressed strongly suggests that the C-terminal half of GCD2 can compete with wild-type GCD2 for complex formation only after forming a trimeric complex with GCD7 and GCN3. Thus, these findings support the idea that GCD2 interacts with GCD7 and GCN3 through the regions of shared sequence similarity in the C-terminal half of GCD2.

DISCUSSION

Evidence that GCD2, GCD7, and GCN3 comprise a regulatory domain required for the inhibition of eIF2B by eIF2(αP). A considerable body of genetic data indicating that the *GCD2*, *GCD7*, and *GCN3* subunits of eIF2B are structurally related and carry out similar functions in mediating the inhibitory effect of eIF2(αP) on eIF2B recycling activity has been obtained. We have isolated point mutations in *GCD2*, *GCD7*, and *GCN3* that make eIF2B completely insensitive to eIF2 phosphorylation without having a detectable effect on eIF2B catalytic activity (27, 35). These Gcn$^-$ regulatory mutations map to similar locations in GCD2, GCD7, and GCN3, and some alter homologous residues in two or even all three proteins, suggesting that homologous structural elements in GCD2, GCD7, and GCN3 carry out related functions in the regulation of eIF2B by eIF2(αP) (27). To explain these findings, we proposed that GCD7, GCN3, and the C-terminal half of GCD2 directly interact to form a regulatory domain in eIF2B. Some of the homologous segments in these three proteins would mediate specific contacts between eIF2B and eIF2(αP), allowing recognition of phosphoserine at position 51, while others could be involved in distorting the catalytic site in eIF2B when phosphoserine is detected at position 51. Regions of sequence similarity in the three proteins that are devoid of Gcn$^-$ regulatory mutations might stabilize common tertiary structures or mediate the interactions between the subunits (27).

The results presented in this report support several aspects of this hypothesis. Our demonstration that overexpressed GCD2, GCD7, and GCN3 form an eIF2B subcomplex in vivo that can be immunoprecipitated from cell extracts (Fig. 5) provides strong biochemical evidence that these proteins directly interact with one another in eIF2B. Formation of this subcomplex led to a substantial reduction in the growth inhibition associated with high levels of eIF2(αP) by a constitutively activated form of GCN2 (Table 1 and Fig. 1). We concluded that this subcomplex does not possess the ability to catalyze the conversion of eIF2 · GDP to eIF2 · GTP, and its presence actually appears to lower eIF2B activity in *gcn2Δ* cells, in which eIF2(αP) cannot be produced (Fig. 3B). Because the trimeric subcomplex rescued eIF2B function only under conditions under which eIF2B was inhibited by phosphorylation of eIF2, we proposed that it directly interacts with eIF2(αP). According to our model, this interaction decreases the frequency with which eIF2(αP) binds to native eIF2B and thus enables the latter to recycle nonphosphorylated eIF2 at a higher rate (Fig. 10, I to III).

Overexpression of wild-type GCD2 alone or in combination with GCD7 and GCN3 appeared to reduce eIF2B function in a *gcn2Δ* mutant in which there is no eIF2(αP) (Fig. 3B and 8A). We attribute this phenomenon to an imbalance of eIF2B subunits that leads to dissociation of a fraction of eIF2B. For example, overexpression of GCD2 alone could lead to the formation of incomplete complexes containing GCD1 but lacking GCD6, and other subcomplexes containing GCD1 but lacking GCD6, in both cases reducing the abundance of five-subunit eIF2B. The reduction in eIF2B function caused by subunit imbalance should diminish the ability of the GCD2-GCD7-GCN3 subcomplex to rescue eIF2B from inhibition by eIF2(αP). We suggest that in *GCN2^c* mutants, the positive effect of sequestering eIF2(αP) outweighs the negative effect of subunit imbalance in dissociating a fraction of eIF2B. In *gcn2Δ* mutants, in which eIF2(αP) is absent, only the negative effects of subunit imbalance are observed. A corollary of this interpretation is that the ability of the trimeric subcomplex to sequester eIF2(αP) may be underestimated by measurements of growth rate in the *GCN2^c* mutants since growth reflects a balance between the positive and negative effects of overexpressing these three subunits on eIF2B function.

We found that cooverexpressing GCD2 and GCD7 suppressed the slow-growth phenotype of the *GCN2^c* mutant to the same extent as when GCD2, GCD7, and GCN3 were cooverexpressed. However, we were unable to demonstrate high levels of a stable GCD2-GCD7 binary complex in the strain overexpressing these two proteins alone. This led us to suspect that overexpressing only GCD2 and GCD7 suppresses the *GCN2^c* allele by titrating GCN3 from native eIF2B into the trimeric subcomplex, leaving the four-subunit form of eIF2B that is relatively insensitive to eIF2(αP) (9). This conclusion is consistent with the fact that the toxicity of the human eIF2α kinase PKR could not be reduced by overexpression of GCD2 and GCD7 in a strain lacking GCN3 (Fig. 6A). It is also supported by our finding that overexpressing GCD2 and GCD7 reduced the growth-inhibitory effect of *gcn3^c-R104K*, presumably by stripping eIF2B of this inhibitory form of GCN3 and

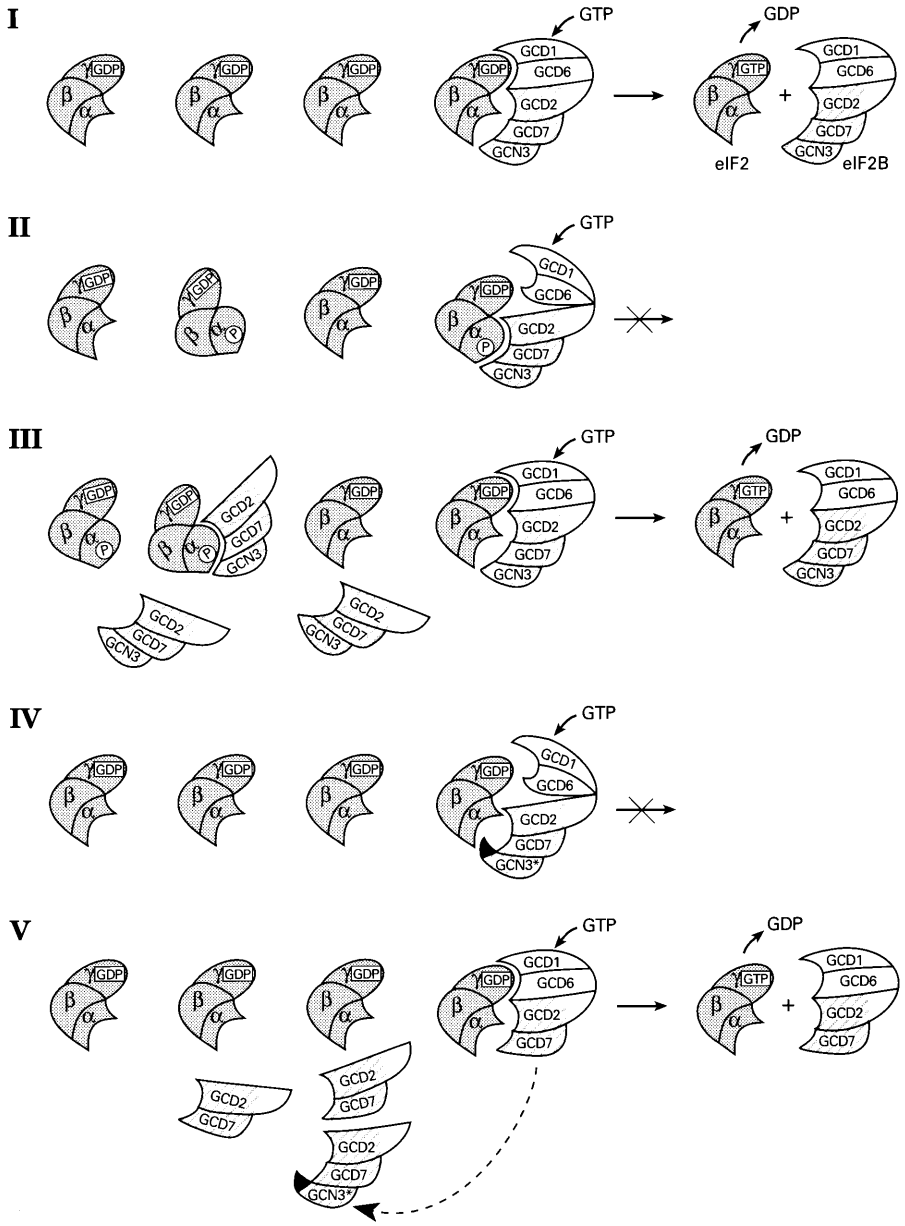

FIG. 10. Model explaining how overexpressing GCD2, GCD7, and GCN3 suppresses the toxicity of eIF2(αP). The heterotrimeric eIF2 complex is shown shaded with a binding site for GDP or GTP on the γ subunit. The eIF2B complex containing GCD1, GCD6, GCD2, GCD7, and GCN3 is shown with GCD7, GCN3, and the C-terminal half of GCD2 identically shaded to reflect similarities in their amino acid sequences. The latter three subunits are grouped together in eIF2B and shown interacting with the α subunit of eIF2 on the basis of their sequence similarities, the mutations isolated in these three subunits that render eIF2B insensitive to eIF2(αP) (27, 35), and the results presented in this report. GCD1 and GCD6 are shown interacting with one another because of sequence similarities between these two subunits (3); the idea that they comprise the active site in eIF2B is hypothetical. The fact that the γ subunit of eIF2 (encoded by *GCD11*) contains sequence motifs involved in GTP binding and hydrolysis conserved among GTP-binding translation factors (e.g., EF-Tu) leads to the prediction that GCD11 contains the GTP-binding site on eIF2; therefore, it is shown interacting with the active site of eIF2B. I, the exchange of GDP for GTP on eIF2 is catalyzed by eIF2B. II, the α subunit of eIF2 has been phosphorylated on Ser-51 by GCN2 in 50% of the eIF2 molecules. Phosphorylated eIF2 is an inhibitor of eIF2B, shown here distorting the hypothetical active site formed by the GCD1 and GCD6 subunits. This prevents the recycling of unphosphorylated eIF2. III, overexpression of GCD2, GCD7, and GCN3 leads to the formation of an eIF2B subcomplex that can interact with eIF2(αP) and prevent it from binding to native eIF2B. This permits the latter to catalyze nucleotide exchange on nonphosphorylated eIF2. IV, the *gcn3^c-R104K* mutation alters GCN3 and the eIF2B complex in a way that mimics the inhibitory effect of eIF2(αP) on the eIF2B active site, preventing recycling of nonphosphorylated eIF2. V, overexpression of GCD2 and GCD7 titrates the *gcn3^c-R104K* protein from eIF2B into the eIF2B subcomplex, yielding the four-subunit form of eIF2B that is competent to recycle eIF2.

sequestering it in trimeric complexes with GCD2 and GCD7 (Fig. 10, IV and V). The fact that overexpressing GCD2 and GCD7 lessened the toxicity of *gcn3^c-R104K* provides independent evidence that GCD2, GCD7, and GCN3 can form a stable subcomplex in vivo.

Essentially all of the eIF2B in the cell is found complexed with eIF2 (8); however, only a fraction of eIF2 coimmunoprecipitates with eIF2B because the latter is present at 8- to 10-fold-lower amounts than is eIF2 (8) (Fig. 5). If the GCD2-GCD7-GCN3 subcomplex and native eIF2B formed equally stable complexes with eIF2, then we might expect to find a larger fraction of eIF2α coimmunoprecipitating with GCD2

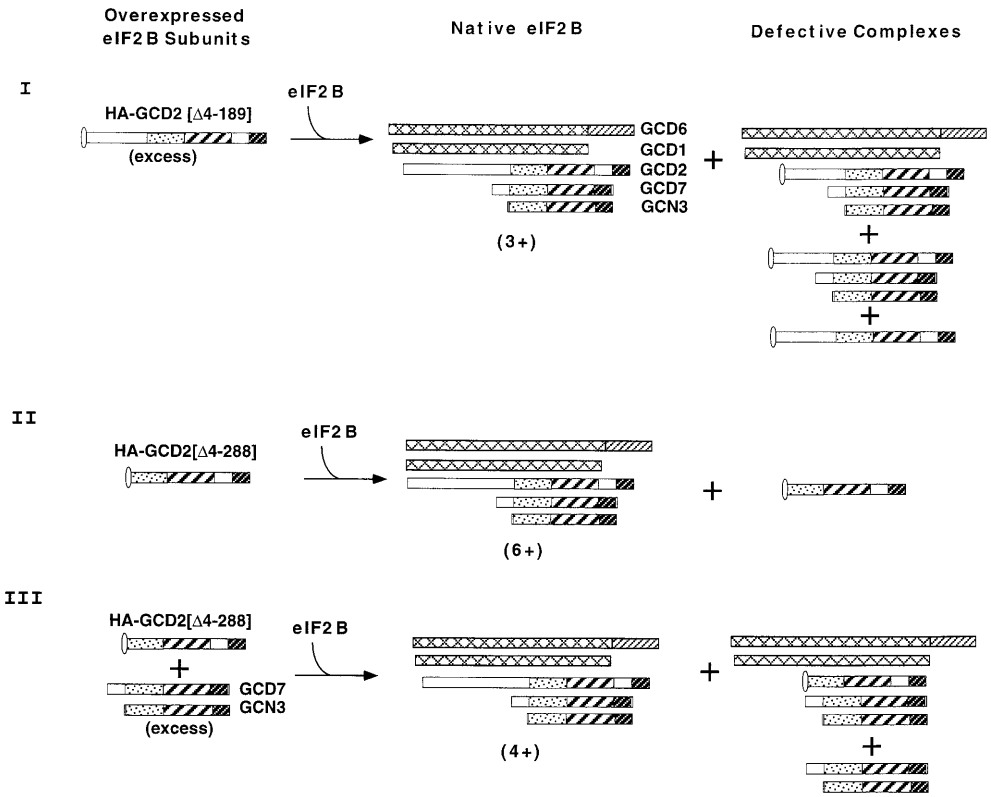

FIG. 11. Proposed effects of expressing N-terminally truncated GCD2 proteins on eIF2B complex formation. Each panel depicts schematically the truncated HA-tagged GCD2 protein that is being expressed in yeast cells (shown on the far left) either alone (I and II) or in combination with GCD7 and GCN3 (III) and the defective eIF2B subcomplexes that are expected to be present (shown on the far right), as determined from the immunoprecipitation experiments shown in Fig. 9. The defective subcomplexes are generated by dissociation of native eIF2B, and the approximate amount of the wild-type complex predicted to remain is indicated by the number (3+, 6+, or 4+) given in parentheses under the schematic for native eIF2B in each panel. These estimates are based on the degree of 3-AT resistance observed in *gcn2*Δ strains expressing the proteins indicated on the left (see the legend to Fig. 8 and text for details). The common shading used for the various subunits indicates regions of sequence similarity between GCD1 and GCD6 or among GCD2, GCD7, and GCN3. N-terminally truncated GCD2 proteins bearing the HA tag are shown with an oval attached to the N terminus, which designates the tag.

from strains overexpressing GCD2, GCD7, and GCN3 than in wild-type strains. Instead, we saw no increase in the fraction of eIF2α that coimmunoprecipitated with GCD2 when GCD2, GCD7, and GCN3 were cooverexpressed (Fig. 5). One possible explanation for this result could be that the trimeric complex stably interacts only with phosphorylated eIF2, while the experiments in Fig. 5 were carried out in a wild-type *GCN2* strain under nonstarvation conditions wherein most eIF2 is not phosphorylated on Ser-51 (10). To address this possibility, we repeated the coimmunoprecipitation experiments in a strain containing a *GCN2*^{c} allele in which a substantial proportion of the eIF2 is phosphorylated (10). However, we observed the same small fraction of eIF2 coimmunoprecipitating with GCD2 when GCD2, GCD7, and GCN3 were overexpressed in the *GCN2*^{c} mutant that was seen when GCD2 was immunoprecipitated from wild-type cells (data not shown). To explain these negative results, we propose that eIF2(αP) interacts with the trimeric subcomplex either with a lower affinity or with an increased off rate compared with its interaction with native eIF2B, such that the hypothetical complex between eIF2(αP) and the trimeric subcomplex dissociated during our coimmunoprecipitation experiments. This is not unreasonable considering that GCD6 and GCD1 are required for the catalytic function of eIF2B and thus probably interact with the predicted GTP-binding site on the γ subunit of eIF2 (15). These additional interactions could make important contributions to the stability of the eIF2 · eIF2B complex and would be lacking in the hypothetical complex between eIF2(αP) and the trimeric subcomplex.

The N-terminal half of GCD2 is essential for eIF2B function but dispensable for complex formation. We found that deleting N-terminal residues 4 to 189 of GCD2 and overexpressing the truncated protein led to a reduction in eIF2B activity (Fig. 8A). This dominant-negative phenotype can be explained by proposing that the HA-GCD2(Δ4-189) protein competes with native GCD2 for complex formation and produces a catalytically defective form of eIF2B. This interpretation is supported by the fact that a fraction of the GCD1, GCD6, GCD7, and GCN3 can be coimmunoprecipitated with the Δ4-189 protein from strains overexpressing only this truncated form of GCD2 (Fig. 9, lanes 8 and 9). From the proportions of GCD1, GCD6, and GCD7 that were immunoprecipitated with HA-GCD2(Δ4-189) in several independent experiments, we estimated that at least one-third of the GCD7 and one-sixth of the GCD1 and GCD6 were associated with HA-GCD2(Δ4-189) in vivo (see the legend to Fig. 9). On the basis of these proportions of coimmunoprecipitated proteins, we predict that one-third or more of the eIF2B complexes are defective, and these include five-subunit complexes containing HA-GCD2(Δ4-189) and trimeric HA-GCD2(Δ4-189)–GCD7–GCN3 complexes in roughly equal proportions (Fig. 11, I).

A more extensively truncated GCD2 protein lacking residues 4 to 288 had a similar dominant-negative phenotype when expressed in cells overproducing GCD7 and GCN3 but not

when expressed alone (Fig. 8A). The Δ4-288 protein accumulated to much lower levels than did the Δ4-189 protein (Fig. 8B) and was present at amounts comparable to that of wild-type GCD2 expressed from the chromosomal allele. Overexpression of GCD7 and GCN3 led to a modest increase in abundance of the Δ4-288 protein (Fig. 9) but, more importantly, allowed the Δ4-288 protein to complex with a fraction of GCD1 and GCD6 as well as with GCD7 and GCN3 (Fig. 9, lanes 3 and 6). We estimated that at least one-sixth of the GCD1 and GCD6 was associated with the Δ4-288 protein in strains overexpressing GCD7 and GCN3 (Fig. 9 legend), presumably forming defective five-subunit complexes containing the Δ4-288 truncation (Fig. 11, III). When GCD7 and GCN3 were not in excess, the HA-GCD2(Δ4-288) protein had no effect on the level of the native five-subunit complex (Fig. 11, II).

The fact that the 4-288Δ truncation of GCD2 can interact with GCD1 and GCD6 only when GCD7 and GCN3 are overexpressed can be explained by proposing that this truncated protein cannot effectively compete with native GCD2 for complex formation because it lacks the ability to make strong contacts with GCD1, GCD6, or GCD7; consequently, it exists in monomeric form when it must compete with native GCD2 for interaction with these other subunits (Fig. 11, II). When GCD7 and GCN3 are in excess, however, the Δ4-288 protein can complex with these two subunits without having to compete with wild-type GCD2, and the resulting trimeric subcomplex can titrate a fraction of GCD1 and GCD6 from native eIF2B into an inactive five-subunit complex (Fig. 11, II). Presumably, the HA-GCD2(Δ4-288)–GCD7–GCN3 trimeric complex can make more contacts with GCD1 and GCD6 than any of its components can make individually.

Our finding that HA-GCD2(Δ4-288) can physically interact with the other subunits of eIF2B (Fig. 9) indicates that the C-terminal 55% of GCD2 (residues 289 to 651) is sufficient for complex formation. Our finding that overexpressing GCD7 and GCN3 is required for the Δ4-288 protein to interact with other eIF2B subunits strongly suggests that the Δ4-288 truncation can form a ternary complex with GCD7 and GCN3. These results are in accordance with our previous proposal that GCD2, GCD7, and GCN3 interact through regions of sequence similarity, as the homologous segments in GCD2 are located C terminal to position 288 (Fig. 11). In addition, all nine regulatory mutations obtained in *GCD2* which render eIF2B less sensitive to the inhibitory effects of eIF2(αP) map in these homologous regions, indicating that the C-terminal half of GCD2 is both functionally and structurally related to GCD7 and GCN3 (27). In future studies, we hope to identify specific residues in GCD2, GCD7, and GCN3 involved in the interactions among these three proteins in the trimeric subcomplex, and also the interactions with GCD1 and GCD6 and the subunits of eIF2 that mediate regulation of eIF2B by phosphorylated eIF2.

ACKNOWLEDGMENTS

We thank Graham Pavitt and Patrick Romano for gifts of strains, and we thank Graham Pavitt and Thomas Dever for helpful suggestions and comments on the manuscript.

REFERENCES

1. **Bradford, M. M.** 1976. A rapid and sensitive method for the quantitation of microgram quantities of protein utilizing the principle of protein-dye binding. Anal. Biochem. **72:**248–254.
2. **Burnette, W.** 1981. "Western blotting": electrophoretic transfer of proteins from sodium dodecyl sulfate-polyacrylamide gels to unmodified nitrocellulose and radiographic detection with antibody and radioiodinated protein A. Anal. Biochem. **112:**195–203.
3. **Bushman, J. L., A. I. Asuru, R. L. Matts, and A. G. Hinnebusch.** 1993. Evidence that GCD6 and GCD7, translational regulators of *GCN4*, are subunits of the guanine nucleotide exchange factor for eIF-2 in *Saccharomyces cerevisiae*. Mol. Cell. Biol. **13:**1920–1932.
4. **Bushman, J. L., M. Foiani, A. M. Cigan, C. J. Paddon, and A. G. Hinnebusch.** 1993. Guanine nucleotide exchange factor for eIF-2 in yeast: genetic and biochemical analysis of interactions between essential subunits GCD2, GCD6, and GCD7 and regulatory subunit GCN3. Mol. Cell. Biol. **13:**4618–4631.
5. **Chong, K. L., L. Feng, K. Schappert, E. Meurs, T. F. Donahue, J. D. Friesen, A. G. Hovanessian, and B. R. G. Williams.** 1992. Human p68 kinase exhibits growth suppression in yeast and homology to the translational regulator GCN2. EMBO J. **11:**1553–1562.
6. **Christianson, T. W., R. S. Sikorski, M. Dante, J. H. Shero, and P. Hieter.** 1992. Multifunctional yeast high-copy-number shuttle vectors. Gene **110:** 119–122.
7. **Cigan, A. M., J. L. Bushman, T. R. Boal, and A. G. Hinnebusch.** 1993. A protein complex of translational regulators of *GCN4* is the guanine nucleotide exchange factor for eIF-2 in yeast. Proc. Natl. Acad. Sci. USA **90:**5350–5354.
8. **Cigan, A. M., M. Foiani, E. M. Hannig, and A. G. Hinnebusch.** 1991. Complex formation by positive and negative translational regulators of *GCN4*. Mol. Cell. Biol. **11:**3217–3228.
9. **Dever, T. E., J. J. Chen, G. N. Barber, A. M. Cigan, L. Feng, T. F. Donahue, I. M. London, M. G. Katze, and A. G. Hinnebusch.** 1993. Mammalian eukaryotic initiation factor 2α kinases functionally substitute for GCN2 in the *GCN4* translational control mechanism of yeast. Proc. Natl. Acad. Sci. USA **90:**4616–4620.
10. **Dever, T. E., L. Feng, R. C. Wek, A. M. Cigan, T. D. Donahue, and A. G. Hinnebusch.** 1992. Phosphorylation of initiation factor 2α by protein kinase GCN2 mediates gene-specific translational control of *GCN4* in yeast. Cell **68:**585–596.
11. **Dever, T. E., W. Yang, S. Astrom, A. S. Bystrom, and A. G. Hinnebusch.** 1995. Modulation of $tRNA_i^{Met}$, eIF-2, and eIF-2B expression shows that *GCN4* translation is inversely coupled to the level of eIF-2 · GTP · Met-$tRNA_i^{Met}$ ternary complexes. Mol. Cell. Biol. **15:**6351–6363.
12. **Garcia-Barrio, M. T., T. Naranda, R. Cuesta, A. G. Hinnebusch, J. W. B. Hershey, and M. Tamame.** 1995. GCD10, a translational repressor of *GCN4*, is the RNA-binding subunit of eukaryotic translation initiation factor-3. Genes Dev. **9:**1781–1796.
13. **Green, N., H. Alexander, A. Olson, S. Alexander, T. M. Shinnick, J. G. Sutcliffe, and R. A. Lerner.** 1982. Immunogenic structure of the influenza virus hemagglutinin. Cell **28:**477–487.
14. **Hannig, E. H., N. P. Williams, R. C. Wek, and A. G. Hinnebusch.** 1990. The translational activator GCN3 functions downstream from GCN1 and GCN2 in the regulatory pathway that couples *GCN4* expression to amino acid availability in *Saccharomyces cerevisiae*. Genetics **126:**549–562.
15. **Hannig, E. M., A. M. Cigan, B. A. Freeman, and T. G. Kinzy.** 1992. *GCD11*, a negative regulator of *GCN4* expression, encodes the gamma subunit of eIF-2 in *Saccharomyces cerevisiae*. Mol. Cell. Biol. **13:**506–520.
16. **Hill, D. E., and K. Struhl.** 1988. Molecular characterization of *GCD1*, a yeast gene required for general control of amino acid biosynthesis and cell-cycle initiation. Nucleic Acids Res. **16:**9253–9265.
17. **Hinnebusch, A. G.** 1992. General and pathway-specific regulatory mechanisms controlling the synthesis of amino acid biosynthetic enzymes in *Saccharomyces cerevisiae*, p. 319–414. *In* E. W. Jones, J. R. Broach, and T. R. Pringle (ed.), The molecular and cellular biology of the yeast *Saccharomyces*: gene expression. Cold Spring Harbor Laboratory Press, Cold Spring Harbor, N.Y.
18. **Hinnebusch, A. G.** 1993. Gene-specific translational control of the yeast *GCN4* gene by phosphorylation of eukaryotic initiation factor 2. Mol. Microbiol. **10:**215–223.
19. **Hinnebusch, A. G.** 1994. The eIF-2α kinases: regulators of protein synthesis in starvation and stress. Cell Biol. **5:**417–426.
20. **Hinnebusch, A. G.** 1994. Translational control of *GCN4*: an *in vivo* barometer of initiation factor activity. Trends Biochem. Sci. **19:**409–414.
21. **Hinnebusch, A. G.** 1996. Translational control of *GCN4*: gene-specific regulation by phosphorylation of eIF2, p. 199–244. *In* J. W. B. Hershey, M. B. Mathews, and N. Sonenberg (ed.), Translational control. Cold Spring Harbor Laboratory Press, Cold Spring Harbor, N.Y.
22. **Ito, H., Y. Fukada, K. Murata, and A. Kimura.** 1983. Transformation of intact yeast cells treated with alkali cations. J. Bacteriol. **153:**163–168.
23. **Jones, E. W.** 1991. Tackling the protease problem in *Saccharomyces cerevisiae*. Methods Enzymol. **194:**428–453.
24. **Koerner, T. J., J. E. Hill, A. M. Myers, and A. Tzagoloff.** 1991. High-expression vectors with multiple cloning sites for construction of *trpE* fusion genes: pATH vectors. Methods Enzymol. **194:**477–490.
25. **London, I. M., D. H. Levin, R. L. Matts, N. S. B. Thomas, R. Petryshyn, and J. J. Chen.** 1987. Regulation of protein synthesis, p. 359–380. *In* P. D. Boyer and E. G. Krebs (ed.), The enzymes, vol. 18. Academic Press, New York.
26. **Paddon, C. J., E. M. Hannig, and A. G. Hinnebusch.** 1989. Amino acid sequence similarity between GCN3 and GCD2, positive and negative trans-

lational regulators of *GCN4*: evidence for antagonism by competition. Genetics **122:**551–559.
27. **Pavitt, G. D., W. Yang, and A. G. Hinnebusch.** Identification of amino acids in homologous segments of 3 subunits of the guanine nucleotide exchange factor eIF2B required for translational regulation by phosphorylation of eukaryotic translation initiation factor 2. Submitted for publication.
28. **Ramirez, M., R. C. Wek, C. R. Vazquez de Aldana, B. M. Jackson, B. Freeman, and A. G. Hinnebusch.** 1992. Mutations activating the yeast eIF-2α kinase GCN2: isolation of alleles altering the domain related to histidyl-tRNA synthetases. Mol. Cell. Biol. **12:**5801–5815.
28a. **Romano, P., and A. G. Hinnebusch.** Unpublished data.
29. **Rose, M. D., F. Winston, and P. Hieter.** 1990. Methods in yeast genetics. Cold Spring Harbor Laboratory Press, Cold Spring Harbor, N.Y.
30. **Rowlands, A. G., R. Panniers, and E. C. Henshaw.** 1988. The catalytic mechanism of guanine nucleotide exchange factor action and competitive inhibition by phosphorylated eukaryotic initiation factor 2. J. Biol. Chem. **263:**5526–5533.
31. **Sanger, F., S. Nicklen, and A. R. Coulson.** 1977. DNA sequencing with chain-terminating inhibitors. Proc. Natl. Acad. Sci. USA **74:**5463–5467.
32. **Sherman, F., G. R. Fink, and C. W. Lawrence.** 1974. Methods of yeast genetics. Cold Spring Harbor Laboratory, Cold Spring Harbor, N.Y.
33. **Sikorski, R. S., and P. Hieter.** 1989. A system of shuttle vectors and yeast host strains designed for efficient manipulation of DNA in *Saccharomyces cerevisiae*. Genetics **122:**19–27.
34. **Taylor, S. S.** 1989. cAMP-dependent protein kinase. Model for an enzyme family. J. Biol. Chem. **264:**8443–8446.
35. **Vazquez de Aldana, C. R., and A. G. Hinnebusch.** 1994. Mutations in the GCD7 subunit of yeast guanine nucleotide exchange factor eIF-2B overcome the inhibitory effects of phosphorylated eIF-2 on translation initiation. Mol. Cell. Biol. **14:**3208–3222.